Structures, Bond Energies, Heats of Formation, and Quantitative Bonding Analysis of Main-Group Metallocenes [E(Cp)$_2$] (E = Be – Ba, Zn, Si – Pb) and [E(Cp)] (E = Li – Cs, B – Tl)**

Víctor M. Rayón and Gernot Frenking*[a]

Abstract: The geometries, metal – ligand bond dissociation energies, and heats of formation of twenty sandwich and half-sandwich complexes of the main-group elements of Groups 1, 2, 13, and 14, and Zn have been calculated with quantum chemical methods. The geometries of the [E(Cp)] and [E(Cp)$_2$] complexes were optimized using density functional theory at the BP86 level with valence basis sets, which have DZP and TZP quality. Improved energy values have been obtained by using coupled-cluster theory at the CCSD(T) level. The nature of the metal – ligand bonding has been analyzed with an energy-partitioning method. The results give quantitative information about the strength of the covalent and electrostatic interactions between E^{n+} and $(Cp^-)_n$ ($n = 1, 2$). The contributions of the orbitals with different symmetry to the covalent bonding are also given.

Keywords: bond energy · bonding analysis · density functional calculations · heats of formation · metallocenes

Introduction

The synthesis of the first sandwich complex ferrocene [Fe(Cp)$_2$], which was published by Kealy and Pauson fifty years ago,[1, 2] is considered as a landmark event in organometallic chemistry.[3] It was the starting point for a new class of compounds called metallocenes that became ubiquitious in synthetic[4] and industrial[5] applications. The initial suggestion of the structure having two Fe–C_5H_5 σ bonds[1] was soon corrected in two independent publications by Fischer and Pfab[6] and by Wilkinson, Rosenblum, Whiting, and Woodward,[7] who showed that the molecule has a π-bonded sandwich structure. A bonding model for ferrocene using symmetry-adapted molecular orbitals, which is also valid for other metallocenes of the transition metals, was introduced by Shustorovich and Dyatkina.[8] The orbital correlation model is now generally accepted and used as a standard in many textbooks.[9] The metal – ligand bonding is explained in terms of donor – acceptor interactions between Fe^{2+} (t_{2g}, d^6) and two Cp^- ligands. A recent energy-partitioning analysis of ferrocene showed that the [$Fe^{2+}(Cp^-)_2$] bonding is ≈51 % electrostatic and ≈49 % covalent, and that two thirds of the covalent interactions come from $(Cp^-)_2 \rightarrow Fe^{2+}$ π donation of the e_{1g} MO of the ligand into the degenerate d(π) metal orbitals.[10]

Metallocenes have in the meantime also been synthesized with main-group elements E, which may be metals or other atoms. Although the term metallocene was originally defined for sandwich compounds [E(Cp)$_2$], in which E is a metal, it is now also used for compounds with only one Cp ligand [E(Cp)] and for complexes with main-group elements E such as silicon and boron. Recent reviews of main-group metallocenes show that a large number of compounds with the formula [E(Cp)] and [E(Cp)$_2$], particularly with elements E of the Groups 1, 2, 13, 14, and 15, have been synthesized and structurally characterized by X-ray analysis.[11] Numerous quantum chemical calculations of main-group metallocenes have also been published in recent years. The theoretical knowledge, which has been gained in these studies, was recently reviewed by Kwon and McKee.[12] Many calculations have been aimed at determining the equilibrium geometry of [E(Cp)$_2$] compounds which may have parallel (D_{5d}, D_{5h}) or bent (C_{2v}, C_s, C_2) structures (Scheme 1). The bonding situation in the compounds has also been analyzed with qualitative bonding models. There is general agreement that, in main-group metallocenes, π-type interactions are weaker than in transition-metal metallocenes because the main-group elements do not have d-type valence orbitals.[11, 12] The bonding of the Cp ligand to the s-block elements (Groups 1, 2) is considered to be mainly ionic, while complexes of the p-block elements should be predominantly covalent. Therefore, orbital correlation diagrams of main-group metallocenes use only the s and p orbitals of E for a discussion of the covalent bonding in [E(Cp)] and [E(Cp)$_2$] complexes.[11, 12]

[a] Prof. G. Frenking, Dr. V. M. Rayón
Fachbereich Chemie, Philipps-Universität Marburg
Hans-Meerwein-Strasse, 35032 Marburg (Germany)
Fax: (+49) 6421-2825566
E-mail: frenking@chemie.uni-marburg.de

[**] Theoretical Studies of Organometallic Compounds, Part 47; For Part 46 see: A. Kovacs, G. Frenking, *Organometallics* **2001**, *20*, 2510.

  0947-6539/02/0820-4693 $ 20.00+.50/0

Scheme 1. Representation of the parallel (also called linear) and bent form of metallocenes $[E(Cp)_2]$. Depending on the rotation about the E–Cp bond axis, the parallel form may have D_{5d} (staggered) or D_{5h} (eclipsed) symmetry, and the bent form may have C_{2v}, C_s, C_2, or C_1 symmetry.

It would be very helpful if the covalent and electrostatic contributions to the E–Cp bonding and the strength of the different orbital terms could be quantitatively given. The recent review by Kwon and McKee recognized this by saying: "there is not enough data from high-level theoretical calculations to have a quantitative understanding of the factors involving covalent or ionic bonding between the Cp ligand and the main-group element".[13] We have given such data for transition-metal metallocenes in our analysis of the bonding in ferrocene $[Fe(Cp)_2]$ and isoelectronic iron bispentazole $[Fe(\eta^5\text{-}N_5)_2]$[10a] and in the homoleptic and heteroleptic complexes with the heavier Group 15 analogues $[Fe(\eta^5\text{-}E_5)_2]$ and $[Fe(Cp)(\eta^5\text{-}E_5)]$.[10b] The studies are part of our ongoing theoretical work, which aims at a systematic quantitative analysis of chemical bonding in main-group and transition-metal compounds that gives the strength of the covalent and electrostatic bonding and of the contributions by the orbitals having different symmetry.[10, 14] It is our goal to compare the chemical bonds of different elements and different structures in a quantitative fashion by using accurate quantum chemical methods. In this paper we present results for the main-group metallocenes $[E(Cp)_2]$ (E = Be – Ba, Si – Pb) and [E(Cp)] (E = Li – Cs, B – Tl). We present for the first time bond dissociation energies and heats of formation of all molecules. The bonding analysis uses the energy-partitioning scheme in the program ADF,[15] which is based on the methods suggested by Morokuma[16] and Ziegler.[17] A short outline is given in the method section.

The following theoretical results are presented for the first time in this paper.

1) A complete set of bond dissociation energies.
2) A complete set of heats of formation.
3) Quantitative analyses of the metal – Cp bonds.

Methods: Nonlocal density functional theory (DFT) using Becke's exchange functional[18] and the correlation functional of Perdew[19] (BP86) was employed to carry out the geometry optimizations. An extra tight grid having 99 radial shells and 590 angular points per shell was used throughout. All the structures located on the potential energy surface (PES) have been characterized by checking the number of negative eigenvalues of the corresponding Hessian matrix. A convergence in the maximum gradient of, at least, 5×10^{-5} hartree bohr^{-1} was achieved. The following basis sets which are labeled in the papers as basis set A have been used. For main-group elements up to the fourth period a standard 6-31G(d) basis set with six cartesian d-type polarization functions was employed.[20, 21] Notice that the 3d shell is included in the valence space of the elements of the fourth period.[21] For the heavier elements of Group 1 (Rb, Cs) a quasirelativistic 9-valence electron (VE) pseudopotential has been used with a (31111/3111/1) valence basis set.[22] We have also used this basis set for K in order to compare the results with the pseudopotential and the 6-31G(d) full electron basis set. The exponents for the six cartesian d-type polarization functions have been optimized in conjunction with the small-core effective core potentials (ECPs) for the interaction of the metal with a cyclopentadienyl ligand, $[M(C_5H_5)]$. The energy-optimized exponents are: $\alpha_d(K) = 0.31$, $\alpha_d(Rb) = 0.22$, and $\alpha_d(Cs) = 0.18$. For the heavier atoms of Group 2 (Ca, Sr, Ba), a quasirelativistic 10-valence electron pseudopotential has been used with a (3111/3111/32) valence basis set for Ca and Sr and a (3111/3111/32/1) valence basis set for Ba.[23] A quasirelativistic 3-VE-ECP has been used for the elements Ga, In, and Tl, and a 4-VE-ECP for the atoms Ge, Sn, and Pb. The valence basis sets for these six elements have (31/31/1) quality.[24] The exponents of the cartesian d-type polarization functions in Ga, In, Ge, and Sn are taken from Huzinaga.[25] For the Zn atom, a relativistic 20-VE ECP has been employed with a (311111/22111/411) basis set.[26] The geometry optimizations have been carried out using the program package Gaussian 98.[27]

In order to improve the calculated energies, CCSD(T)[28, 29] single point calculations were accomplished with a larger basis set B at BP86/A optimized geometries by using the program MOLPRO.[30] In the case of open-shell fragments, we used the RHF-UCCSD(T)[31] method. Basis set B has 6-311G(2d) basis sets[32, 33] for H, Li, Be, B, C, Na, Mg, Al, and Si. Three and four valence electrons have been correlated on atoms belonging to Groups 1 and 13, and 2 and 14, respectively, except Na and Mg, for which nine and ten electrons have been considered. On the other hand, the ten 1s core orbitals of the carbon atoms in the Cp rings have been "frozen" in the correlated calculations. The valence basis sets of the 9-VE-ECP for K, Rb, and Cs have (311111/31111/11) quality, in which the exponents of the outermost s and p valence orbitals are 65 % of the former outermost ones. One set of spherical d-type polarization exponents has been optimized for the 9-valence electron pseudopotential at the CISD level in atomic calculations. The exponents are: $\alpha_d(K) = 1.02$, $\alpha_d(Rb) = 0.57$, and $\alpha_d(Cs) = 0.38$. For the CCSD(T) calculations, each exponent has been split into two following the pattern $2 \cdot \alpha_d$, $\alpha_d/2$. The 10-VE basis sets for Ca and Sr have (31111/31111/21111) quality. Again, the outermost s and p valence orbitals have exponents, which are 65 % smaller than the former outermost ones. The d orbital space, on the other hand, has been re-contracted as indicated, and the outermost d valence orbitals have been split as described above. The valence basis set of Ba has the same contraction scheme and has been augmented with one set of f-type polarization functions. For the atoms of Groups 13 and 14 (Ga, In, and Tl, and Ge, Sn, and Pb), a (211/211/11) basis set has been used. Finally, the basis set employed for the Zn atom has (311111/22111/3111/1) quality, for which we have employed one set of f-type polarization functions with exponent $\alpha_f(Zn) = 4.3$ optimized at the CISD level. All valence electrons apart from the 1s carbon orbitals of the Cp rings have been correlated in the CCSD(T) calculations when using ECPs. Unless otherwise noted, energies will be discussed at CCSD(T)/B and geometries at BP86/A.

0947-6539/02/0820-4694 $ 20.00+.50/0 *Chem. Eur. J.* **2002**, *8*, No. 20

In order to carry out the energy-partitioning analysis, which is described below, the geometries were also optimized with the program package ADF(2000.02)[15, 34] using the BP86 functionals. A convergence threshold for the maximum gradient of 5×10^{-5} hartree bohr^{-1} has been used throughout. Relativistic effects were considered in those compounds having elements of the fifth and sixth period by means of the zero-order regular approximation (ZORA).[35] Uncontracted Slater-type orbitals (STO) were employed as basis functions for the SCF calculations.[36] The (full) basis sets for the main-group elements up to the fourth period have triple-ξ quality augmented by one set of d-type polarization functions. One set of p polarization functions has been added to H. Regarding the main-group atoms of the fifth period, the (1s2s2p3s3p3d)[28] core electrons of Rb and Sr were treated by the frozen core approximation, whereas for In and Sn the frozen core approximation was applied to the (1s2s2p3s3p3d4s4p)[36] core electrons. This gives 9, 10, 13, and 14 valence electrons for the Groups 1, 2, 13, and 14, respectively. Extending the valence space in Group 13 and Group 14 to 13 and 14 electrons, respectively, was necessary to achieve results of the same quality as the ones obtained with 3 and 4 valence electrons in G98. The same number of valence electrons was considered for the Group 1, Group 2, Group 13, and Group 14 elements of the sixth period. This gives a (1s2s2p3s3p3d4s4p4d)[46] core for Cs and Ba and a (1s2s2p3s3p3d4s4p4d4f5s5p)[68] core for Tl and Pb. Basis sets of triple-ξ quality have been used for elements of the fifth and sixth period. These basis sets have been augmented with one set of d- and f-type polarization functions except for In, Sn, and Tl, for which only f-type functions are available. An auxiliary set of s, p, d, f, and g STOs was used to fit the molecular densities and to represent the Coulomb and exchange potentials accurately in each SCF cycle.[37]

For the energy-partitioning analysis the interaction energy ΔE_{int} was calculated and decomposed for the bonding between the metal ions E^{2+} and two Cp^- ligands in $[E(Cp)_2]$ and between E^+ and Cp^- in [E(Cp)] in the electronic ground state, respectively. The instantaneous interaction energy ΔE_{int} can be divided into three components [Eq. (1)].

$$\Delta E_{int} = \Delta E_{elstat} + \Delta E_{Pauli} + \Delta E_{orb} \quad (1)$$

ΔE_{elstat} gives the electrostatic interaction energy between the fragments which are calculated with a frozen-electron-density distribution in the geometry of the complex. It can be considered as an estimate of the *electrostatic* contribution to the bonding interactions. The second term in Equation (1) ΔE_{Pauli} gives the repulsive four-electron interactions between occupied orbitals. The last term gives the stabilizing orbital interactions ΔE_{orb}, which can be considered as an estimate of the *covalent* contributions to the bonding. Thus, the ratio $\Delta E_{elstat}/\Delta E_{orb}$ indicates the electrostatic/covalent character of the bond. The latter term can be partitioned further into contributions by the orbitals which belong to different irreducible representations of the interacting system. This makes it possible to calculate, for example, the contributions of σ and π bonding to a covalent multiple bond. Technical details about the energy partitioning method can be found in the literature.[15, 34]

The bond dissociation energy (BDE) ΔE_e is given by the sum of ΔE_{int} and the fragment preparation energy ΔE_{prep} [Eq. (2)].

$$\Delta E_e = \Delta E_{prep} + \Delta E_{int} \quad (2)$$

ΔE_{prep} is the energy which is necessary to promote the fragments from their equilibrium geometry and electronic ground state to the geometry and electronic state which they have in the optimized structure.

Geometries, bond energies, and heats of formation: The geometry optimization of the complexes was carried out first with restricted symmetry-enforcing C_{5v} symmetry for the [E(Cp)] molecules and D_{5d} symmetry for $[E(Cp)_2]$ species. The calculation of the vibrational frequencies revealed that most structures are minima on the PES (number of imaginary frequencies $i = 0$), while some of them are higher order saddle points with $i = 2$ or in the case of $[Zn(Cp)_2]$ with $i = 4$. In those cases we located the energy minima by lowering the symmetry constraints in the geometry optimization. All Group 1 and Group 13 halfsandwich complexes [E(Cp)] have an equilibrium geometry, which has C_{5v} symmetry (structure type **1**). Seven different structure types **2**–**8** were found by us as energy minima for the sandwich complexes $[E(Cp)_2]$. They are shown in Figure 1. Structures **2** and **3** are the high

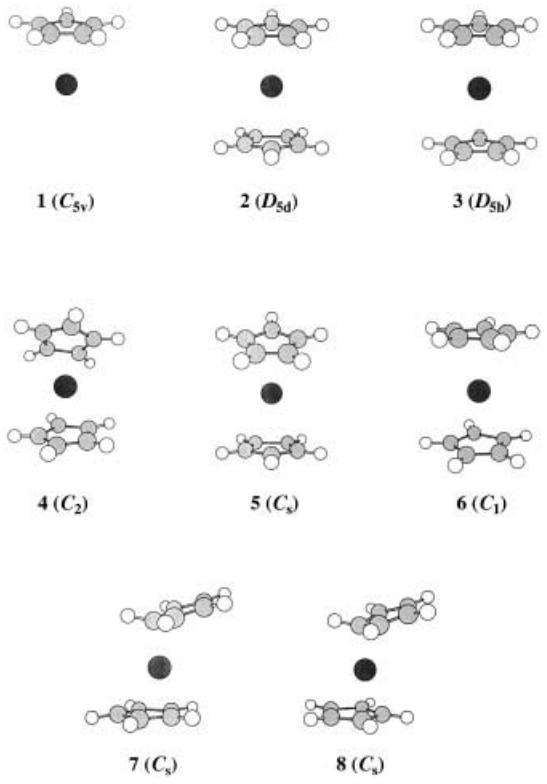

Figure 1. Schematic representation of the structure types **1**–**8**, which have been found as energy minima in this work.

  0947-6539/02/0820-4695 $ 20.00+.50/0

symmetry forms of $[E(Cp)_2]$ with parallel Cp rings, which are staggered (**2**) or eclipsed (**3**). In structures **4**–**6** the Cp rings are bent, that is, the angle X–E–X′ (X, X′ being the center of the Cp rings) is $<180^\circ$. Different rotation of the Cp rings around the E–X and E–X′ axes leads to structures which have C_2 (**4**), C_s (**5**), or C_1 (**6**) symmetry. A bent structure with C_{2v} symmetry was not found as an energy minimum for any of the molecules in this investigation. The binding mode between the metal and the Cp ligands in **1**–**6** is η^5, that is, atom E is bonded to the five carbon atoms. Structures **7** and **8** show "slipped" sandwich complexes $[E(Cp)_2]$, in which the metal binds η^5 to only one ring but in an η^3 to η^1 fashion to the other (**7**) or it binds η^3/η^1 to both rings (**8**). Further details are discussed below.

Table 1 gives the calculated geometries and bond dissociation energies of the investigated metallocenes. The dissociation products have the metal atoms in the respective electronic ground state and the Cp ligand in the $^2B_1$ state. Since the experimental heats of formation of the atoms E and the Cp ligand are known,[38] we took the data and the calculated bond energies in order to predict the ΔH_f^o values of the metallocenes. The results are also shown in Table 1.

We begin the discussion of the results with the alkaline complexes [E(Cp)] (E = Li–Cs). All molecules belong to structure type **1**, that is, they have geometries with C_{5v} symmetry. The calculated bond lengths are very similar to previously reported values of [Li(Cp)][39] and [Na(Cp)],[40] which come from accurate quantum chemical methods.[12] The complexes with E = K, Rb, and Cs have not been calculated by ab initio or DFT methods before. Thus, the data in Table 1 are the first complete set of theoretically predicted geometries and bond energies of Group 1 metallocenes [E(Cp)]. A comparison of the calculated bond lengths with experimental values is not very meaningful because the latter data have been obtained from polymeric compounds or from molecules which carry additional solvent molecules at the metal atom.[11] For example, the measured Cs–X distance (X being the center of the Cp ring) of polymeric [Cs(Cp)] (2.82 Å)[41] is similar to the BP86/A value (2.874 Å), but the agreement is fortuitous and misleading because the measured K–X distance of [K(Cp)] (2.82 Å)[42] is the same as for Cs–X, while the calculated value (2.566 Å) is as expected much shorter.

An interesting result of the energy calculations is that the E–Cp bond strength from Na–Cs remains nearly constant. The cesium complex is predicted to have a rather strong Cs–Cp bond ($D_e = 61.8$ kcal mol^{-1}), which is as strong as the Na–Cp bond ($D_e = 60.8$ kcal mol^{-1}). The Li–Cp bond ($D_e = 86.0$ kcal mol^{-1}) is significantly stronger than the bonds of the heavier analogues. [Li(Cp)] is the only metallocene complex of this work for which the E–Cp bond dissociation energy for the formation of the neutral fragments has been calculated before. Blom et al.[39d] reported the value $D_e = 72.2$ kcal mol^{-1}, which was obtained at the Hartree–Fock level of theory. The calculated bond energy which is given here should be more reliable because the earlier data do not include correlation contributions. We want to point out that the calculated bond energies at BP86/A are very similar to the CCSD(T)/B results. This is gratifying because CCSD(T) calculations are much more expensive to carry out than BP86. The calculated heats of formation of the metallocenes have always positive values. The somewhat irregular trend of the ΔH_f^o values from Li to Cs comes from the data of the atoms E.[38]

Next we discuss the results of the alkaline-earth metallocenes $[E(Cp)_2]$ (E = Be–Ba). Several theoretical studies which report the geometries and electronic structure of the molecules have already been published.[43] The wide variety of experimental and theoretical studies of 14-electron metallocenes has been comprehensively reviewed by Hanusa.[44] The geometry optimization of the D_{5d} geometries at BP86/A yielded structures which are energy minima ($i = 0$) for E = Be, Mg, and Ca but second-order saddle points ($i = 2$) for E = Sr and Ba (Table 1). The calculated geometry of $[Be(Cp)_2]$ is particularly interesting because of experimental data which suggest a rather unusual structure that is still somewhat uncertain.[45] $[Be(Cp)_2]$ has a permanent dipole moment of 2.24 D which clearly shows that the Cp rings cannot be equivalent.[46] The ^{1}H NMR spectrum shows only one signal, however, which indicates a fast exchange of the hydrogen atoms on the NMR timescale.[47] The results of electron diffraction measurements have at first been interpreted as a structure with C_{5v} symmetry which has two η^5-bonded Cp ligands that have different Be–X distances.[48a] A later X-ray structure analysis gave a "slipped sandwich" geometry with approximate C_s symmetry, in which one Cp ligand is η^5-bonded, while the second ring does not lay on top of the first one but it has one short Be–C bond (1.81 Å).[49] A reinterpretation of the electron diffraction data led us to the conclusion that $[Be(Cp)_2]$ may indeed have a slipped-sandwich structure.[48b]

We also optimized the geometry of $[Be(Cp)_2]$ without symmetry constraints by using the experimental geometry as starting point. The calculation yielded a structure with C_s symmetry (Figure 2), which is a minimum on the PES ($i = 0$). At the BP86/A level, the C_s form of $[Be(Cp)_2]$ is 0.1 kcal mol^{-1} lower in energy than the D_{5d} structure. Energy calculations at CCSD(T)/B//BP86/A predict that the former structure is 0.6 kcal mol^{-1} more stable than the latter form. The calculations indicate that the $[Be(Cp)_2]$ PES around the C_s/D_{5d} form is very flat which means that the molecule has a fluxional structure. This is in agreement with the experimental observations.[46–49] The floppiness of the PES must be taken into account when the calculated bond lengths are compared with the experimental values (Figure 2). The calculation suggests that the rings are not coplanar. This may be the reason why the short Be–C distance of the slipped Cp ring is calculated to be much shorter (1.774 Å) than the gas-phase value (1.99 Å). Note that the value from the X-ray structure analysis (1.81 Å) is in much better agreement with the theoretical number than the gas-phase value. The calculated structure shown in Figure 2 suggests that the Be–Cp bonding in $[Be(Cp)_2]$ is best described as η^5/η^1 (structure type **7**). This is in agreement with the latest discussion of the experimental structure.[11b]

We calculated the geometry of $[Mg(Cp)_2]$ with eclipsed Cp rings (D_{5h} symmetry) in addition to the D_{5d} form, because it has been reported that the former conformation prevails in the gas phase,[50] while an X-ray structure analysis identified

  0947-6539/02/0820-4696 $ 20.00+.50/0 *Chem. Eur. J.* **2002**, *8*, No. 20

Table 1. Calculated bond lengths [Å] and angles [°] at BP86/A. Values at BP86/TZP are given in parentheses. Relative energies E_{rel} of the isomers and theoretically predicted bond dissociation energies D_e and ZPE corrected values D_0 [kcal mol^{-1}] at CCSD(T)/B//BP86/A in italics and at BP86/A. Calculated heats of formation ΔH_f^o [kcal mol^{-1}] at CCSD(T)/B//BP86/A.

Molecule	Symm.	E–C	E–X[d]	C–C	β(X–E–X′)[d]	i[g]	E_{rel}	D_e[e]	D_0[e]	ΔH_f^o
[Li(Cp)]	**1** (C_{5v})	2.123	1.740	1.430	–	*0*	–	*– 86.0*	*– 82.3*	*13.4*
		(2.142)	(1.767)	(1.425)				– 82.7	– 79.0	
[Na(Cp)]	**1** (C_{5v})	2.512	2.197	1.430	–	*0*	–	*– 60.8*	*– 58.6*	*25.1*
		(2.524)	(2.214)	(1.425)				– 56.6	– 54.4	
[K(Cp)]	**1** (C_{5v})	2.839	2.566	1.427	–	*0*	–	*– 59.9*	*– 57.9*	*21.6*
		(2.842)	(2.572)	(1.423)				– 52.5	– 50.4	
[Rb(Cp)]	**1** (C_{5v})	3.007	2.751	1.427	–	*0*	–	*– 57.0*	*– 55.3*	*22.3*
		(3.052)	(2.802)	(1.422)				– 52.1	– 50.4	
[Cs(Cp)]	**1** (C_{5v})	3.119	2.874	1.426	–	*0*	–	*– 61.8*	*– 60.0*	*16.5*
		(3.258)	(3.026)	(1.422)				– 57.8	– 56.1	
[Be(Cp)$_2$]	**2** (D_{5d})	2.058	1.661	1.427	180.0	*0*	0.0	*– 161.1*	*– 153.9*	*38.6*
		(2.078)	(1.689)	(1.424)	(180.0)			– 153.9	– 146.6	
[Be(Cp)$_2$]	**7** (C_s)	1.915 – 1.958[a]	1.504[a]	1.430 – 1.432[a]	152.7	*0*	*– 0.6*	*– 161.7*	*– 154.0*	*38.5*
		(1.934 – 1.965)[a]	(1.524)[a]	(1.425 – 1.427)[a]	(153.4)		– 0.1	– 154.0	– 146.3	
		1.774 – 3.064[b]	2.261[b]	1.393 – 1.437[b]						
		(1.777 – 3.189)[b]	(2.355)[b]	(1.383 – 1.437)[b]						
[Mg(Cp)$_2$]	**2** (D_{5d})	2.368	2.030	1.432	180.0	*0*	0.0	*– 127.2*	*– 121.1*	*29.9*
		(2.371)	(2.037)	(1.426)	(180.0)			– 118.7	– 112.5	Exp.: 31 ± 2[f]
[Mg(Cp)$_2$]	**3** (D_{5h})	2.368	2.030	1.432	180.0	*0*	*< + 0.01*	*– 127.2*	*– 121.0*	*30.0*
		(2.371)	(2.038)	(1.426)	(180.0)		< + 0.01	– 118.7	– 112.5	Exp.: 31 ± 2[f]
[Ca(Cp)$_2$]	**2** (D_{5d})	2.645	2.350	1.428	180.0	*0*	0.0	*– 160.3*	*– 154.9*	*3.6*
		(2.668)	(2.377)	(1.423)	(180.0)			– 160.6	– 155.2	
[Sr(Cp)$_2$]	**2** (D_{5d})	2.819	2.544	1.429	180.0	*2*	0.0			
		(2.869)	(2.601)	(1.423)	(180.0)					
[Sr(Cp)$_2$]	**6** (C_1)	2.815 – 2.818[a]	2.541	1.428 – 1.429[c]	167.1	*0*	*+ 0.1*	*– 154.3*	*– 149.3*	*5.7*
		(–)[c]	(–)[c]	(–)[c]	(–)[c]		– 0.02	– 150.3	– 145.3	
[Ba(Cp)$_2$]	**2** (D_{5d})	2.998	2.741	1.428	180.0	*2*	0.0			
		(3.093)	(2.847)	(1.423)	(180.0)					
[Ba(Cp)$_2$]	**5** (C_s)	2.955 – 3.001[a]	2.719	1.427 – 1.428[c]	140.0	*0*	*– 0.2*	*– 166.0*	*– 161.1*	*– 2.1*
		(–)[c]	(–)[c]	(–)[c]	(–)[c]		– 1.2	– 159.2	– 154.3	
[Zn(Cp)$_2$]	**2** (D_{5d})	2.319	1.971	1.436	180.0	*4*	0.0			
		(2.334)	(1.991)	(1.431)	(180.0)					
[Zn(Cp)$_2$]	**8** (C_s)	2.116 – 2.531[a]	2.011[a]	1.425 – 1.450[a]	172.2	*0*	*– 3.7*	*– 74.9*	*– 69.6*	*72.1*
		(2.048 – 2.862)[a]	(2.218)[a]	(1.403 – 1.457)[a]	(177.8)		– 8.8	– 66.2	– 60.9	
		1.986 – 3.332[b]	2.531[b]	1.386 – 1.480[b]						
		(1.998 – 3.307)[b]	(2.520)[b]	(1.382 – 1.473)[b]						
[B(Cp)]	**1** (C_{5v})	2.012	1.607	1.423	–	*0*	–	*– 91.3*	*– 87.3*	*104.0*
		(2.002)	(1.597)	(1.419)				– 99.5	– 94.5	
[Al(Cp)]	**1** (C_{5v})	2.390	2.059	1.428	–	*0*	–	*– 90.7*	*– 87.4*	*49.4*
		(2.396)	(2.068)	(1.423)				– 91.8	– 88.4	
[Ga(Cp)]	**1** (C_{5v})	2.476	2.157	1.429	–	*0*	–	*– 81.3*	*– 78.3*	*44.5*
		(2.471)	(2.154)	(1.424)				– 82.2	– 79.2	
[In(Cp)]	**1** (C_{5v})	2.631	2.333	1.430	–	*0*	–	*– 80.8*	*– 78.0*	*38.2*
		(2.662)	(2.370)	(1.424)				– 79.5	– 76.7	
[Tl(Cp)]	**1** (C_{5v})	2.782	2.502	1.430	–	*0*	–	*– 68.4*	*– 66.0*	*35.7*
		(2.761)	(2.481)	(1.424)				– 69.5	– 67.0	
[Si(Cp)$_2$]	**2** (D_{5d})	2.513	2.201	1.425	180.0	*2*	0.0			
		(2.532)	(2.225)	(1.420)	(180.0)					
[Si(Cp)$_2$]	**4** (C_2)	2.260 – 2.781[a]	2.215	1.415 – 1.440[c]	154.7	*0*	*– 4.6*	*– 130.7*	*– 124.3*	*99.7*
		(2.276 – 2.790)[a]	(2.235)	(1.410 – 1.435)[c]	(155.8)		– 2.8	– 137.4	– 131.0	
[Ge(Cp)$_2$]	**2** (D_{5d})	2.582	2.279	1.427	180.0	*2*	0.0			
		(2.597)	(2.298)	(1.422)	(180.0)					
[Ge(Cp)$_2$]	**5** (C_s)	2.428 – 2.737[a]	2.282	1.419 – 1.435[c]	159.0	*0*	*– 1.0*	*– 123.2*	*– 117.4*	*87.9*
		(2.475 – 2.744)[a]	(2.299)	(1.414 – 1.429)[c]	(162.0)		– 0.6	– 129.3	– 123.4	
[Sn(Cp)$_2$]	**2** (D_{5d})	2.775	2.495	1.428	180.0	*2*	0.0			
		(2.758)	(2.479)	(1.422)	(180.0)					
[Sn(Cp)$_2$]	**5** (C_s)	2.635 – 2.904[a]	2.490	1.420 – 1.435[c]	151.6	*0*	*– 1.7*	*– 116.8*	*– 111.3*	*76.9*
		(2.623 – 2.882)[a]	(2.473)	(1.414 – 1.428)[c]	(154.0)		– 0.9	– 121.5	– 116.0	
[Pb(Cp)$_2$]	**2** (D_{5d})	2.860	2.589	1.429	180.0	*2*	0.0			
		(2.833)	(2.561)	(1.423)	(180.0)					
[Pb(Cp)$_2$]	**6** (C_1)	2.755 – 2.959[a]	2.586	1.423 – 1.433[c]	156.3	*0*	*– 0.5*	*– 111.3*	*– 106.2*	*56.6*
		(2.756 – 2.899)[a]	(2.557)	(1.420 – 1.426)[c]	(163.0)		– 0.3	– 113.0	– 107.9	

[a] Values for the η^5-bonded ring, see Figure 2. [b] Values for the η^1-bonded ring, see Figure 2. [c] Geometry optimization at BP86/TZP leads to the D_{5d} form. [d] X is the center of the ring. [e] Dissociation into atom E and one or two Cp ligands. [f] Reference [55]. [g] Number of imaginary frequencies.

  0947-6539/02/0820-4697 $ 20.00+.50/0

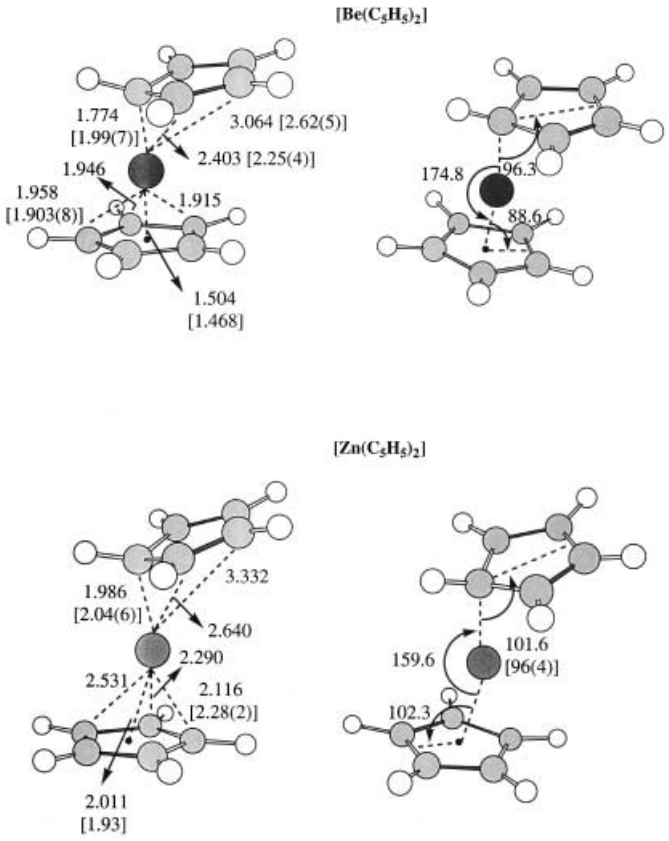

Figure 2. Calculated bond lengths [Å] and angles [°] of $[Be(Cp)_2]$ and $[Zn(Cp)_2]$ at BP86/A. Experimental values are given in brackets.

the latter form in the solid state.[51] The calculations predict that the D_{5h} and D_{5d} forms of magnesocene are energetically nearly degenerate (Table 1). Both conformations are found as minima on the PES. The energy difference between the two forms is only <0.01 kcal mol^{-1}. The heavier metallocenes $[Ca(Cp)_2]$, $[Sr(Cp)_2]$, and $[Ba(Cp)_2]$ in the solid state have bent polymeric structures,[11] and thus, the experimental geometries shall not be compared with the calculated values. Gas-phase values are not available for them. The decamethyl-substituted analogues $[Ca(Cp^*)_2]$, $[Sr(Cp^*)_2]$, and $[Ba(Cp^*)_2]$ are monomeric species, the geometries of which have been measured by electron diffraction[43e, 52] and X-ray structure analysis.[53] The analysis of the recorded data indicated bent sandwich structures with two η^5-bonded Cp rings, but it was pointed out that the molecules might have D_{5d} structures if the energy difference between the parallel and the bent form is <0.5 kcal mol^{-1}.[52] The reported bending angle β(X–E–X′) decreases from E = Ca ($\beta = 154°$) to E = Sr ($\beta = 149°$) and E = Ba ($\beta = 148°$). Table 1 shows that the BP86/A calculations give the same trend for the $[E(Cp)_2]$ species albeit with a steeper decrease. $[Ca(Cp)_2]$ has a linear (D_{5d}) structure, while $[Sr(Cp)_2]$ ($\beta = 167°$) and $[Ba(Cp)_2]$ ($\beta = 140°$) are predicted to be bent. The energy differences between the D_{5d} form and the bent equilibrium structures are very small however. The CCSD(T)/B calculations favor the bent structure of $[Ba(Cp)_2]$ only by 0.2 kcal mol^{-1}, while for $[Sr(Cp)_2]$, the bent form is even 0.1 kcal mol^{-1} higher in energy than the D_{5d} structure. At BP86/TZP, the linear forms of both molecules are found as the energetically lowest lying structures. The geometry optimization of $[Sr(Cp)_2]$ and $[Ba(Cp)_2]$ at BP86/TZP using the bent equilibrium structures as starting points led to the D_{5d} structures. The results presented here agree with previous experimental[4, 11, 44] and theoretical[54] work which suggests that that the alkaline-earth metallocenes have a parallel or quasiparallel structure.

The theoretically predicted bond energies of the alkaline-earth metallocenes are very interesting. The CCSD(T)/B values suggest that $[Ba(Cp)_2]$ has the highest bond energy ($D_e = 166.0$ kcal mol^{-1}) and that $[Be(Cp)_2]$ ($D_e = 161.7$ kcal mol^{-1}) and $[Ca(Cp)_2]$ ($D_e = 160.3$ kcal mol^{-1}) have slightly weaker bonds. Smaller bond energies are calculated for $[Sr(Cp)_2]$ ($D_e = 154.3$ kcal mol^{-1}), but the lowest value is predicted for $[Mg(Cp)_2]$ ($D_e = 127.2$ kcal mol^{-1}). Thus, the trend of the bond energies of the alkaline-earth metallocenes is different from the alkali-metal metallocenes, for which the strongest bond was calculated for the lightest element [Li(Cp)]. The calculated heats of formation of the sandwich complexes of the lighter elements Be and Mg are clearly positive, while the ΔH_f° values of the heavier metallocenes $[Ca(Cp)_2]$, $[Sr(Cp)_2]$, and $[Ba(Cp)_2]$ are close to zero (Table 1). The experimental heat of formation of magnesocene is known.[55] The measured value ΔH_f° ($[Mg(Cp)_2]$) $= 31 \pm 2$ kcal mol^{-1} is in perfect agreement with the calculated result (29.9 kcal mol^{-1}). This means that the theoretical ΔH_f° values and the bond dissociation energies at CCSD(T) should be quite reliable. We want to mention that the heat of formation of magnesocene has previously been calculated by Cioslowski et al. at the B3LYP/6-311++G(d,p) level.[43l] The authors reported the value $\Delta H_f^\circ([Mg(Cp)_2]) = 32.9$ kcal mol^{-1}, which agrees with the experimental result and with our data. The calculated bond dissociation energies of the alkaline-earth metallocenes at BP86/A are always up to 8.5 kcal mol^{-1} lower than the CCSD(T)/B values except for $[Ca(Cp)_2]$, for which the D_e value at the former level is 0.3 kcal mol^{-1} higher than at the latter level (Table 1).

We calculated the structure of $[Zn(Cp)_2]$ which may be compared with the alkaline-earth metallocenes because the electron configuration of Zn ($d^{10}s^2p^0$) resembles those of the elements Be – Ba (s^2p^0). $[Zn(Cp)_2]$ is polymeric in the solid state.[4] Experimental studies suggest that isolated $[Zn(Cp^*)_2]$ has a slipped sandwich geometry and a fluxional structure similar to that found for $[Be(Cp)_2]$.[56] The only previous theoretical work on the geometry of $[Zn(Cp)_2]$ was carried out at the MP2 level of theory.[57a] The optimization was performed with the constraint of D_{5h} symmetry. The vibrational frequencies were not reported, and thus, it is not clear if it is a minimum on the PES. The geometry optimization of the D_{5d} form at BP86/A yielded a structure which has four imaginary frequencies. Calculations with less symmetry constraints indicated a C_s symmetric structure as an energy minimum form ($i = 0$), which is 8.8 kcal mol^{-1} lower in energy than the D_{5d} species. The optimized equilibrium structure is shown in Figure 2. The Cp rings of $[Zn(Cp)_2]$ are not equivalent. The Zn atom has three short (2.116 Å, $2 \times$ 2.290 Å) and two long (2×2.531 Å) Zn–C distances to one Cp ring, while the other Cp ring has one short (1.986 Å) and four long (2×2.640 Å, 2×3.332 Å) Zn–C distances. The

  0947-6539/02/0820-4698 $ 20.00+.50/0 Chem. Eur. J. 2002, 8, No. 20

$Zn-Cp_2$ bonding situation may thus be interpreted as η^3-bonded to one Cp ring and η^1-bonded to the other (structure **8**). However, the distances Zn–C = 2.531 Å of the first ring could still be considered as weak bonds, and this would give one η^5-bonded ring and thus, an 18 electron configuration for Zn. Figure 2 gives also the gas-phase values of $[Zn(Cp^*)_2]$.[56] A comparison of the calculated structure of $[Zn(Cp)_2]$ with the experimental geometry of $[Zn(Cp^*)_2]$ shows a stronger η^5/η^1-bonding situation for the latter complex. The calculated bond energy shows that the $Zn-Cp_2$ bond strength ($D_e = 74.9$ kcal mol^{-1}) is much less than those of the alkaline-earth metallocenes ($D_e = 127.2 - 166.0$ kcal mol^{-1}). The calculated heat of formation of $[Zn(Cp)_2]$ has a strongly positive value (72.1 kcal mol^{-1}).

Now we turn to the Group 13 metallocenes [E(Cp)] (E = B – Tl). The calculations of the geometries gave η^5-bonded structures (C_{5v} symmetry) for all molecules, and this is in agreement with experimental work and with previous theoretical studies.[11, 12, 58] The geometries of the heavier species [In(Cp)] and [Tl(Cp)] have been determined by gas-phase electron diffraction. The experimental In–X distance (2.32 Å) is in excellent agreement with the calculated value (2.333 Å), while the experimental Tl–X value (2.41 Å) is somewhat shorter than the theoretical result (2.502 Å).[11a] Experimental data of the lighter homologues are not known to us, but the geometries of monomeric [Al(Cp*)] and [Ga(Cp*)] have been measured by gas-phase electron diffraction. The reported Al–X value of the former compound (2.06 Å)[59] is the same as the calculated Al–X value of [Al(Cp)] (2.059 Å). The experimental Ga–X bond length of [Ga(Cp*)] (2.08 Å),[60] which is nearly the same as the Al–X bond length in [Al(Cp*)], is shorter than the calculated value for [Ga(Cp)] (2.157 Å). This is reasonable because Cp* is a stronger donor than Cp. However, it is puzzling that [Al(Cp*)] and [Ga(Cp*)] should have nearly the same E–X distances. The calculations predict that the Ga–X bond of [Ga(Cp)] is 0.1 Å longer than the Al–X bond of [Al(Cp)].

The calculated energies (Table 1) predict that [B(Cp)] and [Al(Cp)] have the strongest E–Cp bonds ($D_e = 91$ kcal mol^{-1}) followed by [Ga(Cp)] and [In(Cp)] ($D_e = 81$ kcal mol^{-1}) and [Tl(Cp)] ($D_e = 68$ kcal mol^{-1}). The calculations indicate that the Group 13 metallocenes [B(Cp)] – [Tl(Cp)] have slightly stronger bonds than the Group 1 metallocenes [Li(Cp)] – [Cs(Cp)] of the same period. The theoretically predicted heats of formation of the former species are much more positive particularly for [B(Cp)] because the ΔH_f^o(E) values of the Group 13 atoms have large positive values.[38]

Finally we discuss the results of the Group 14 metallocenes $[E(Cp)_2]$ (E = Si – Pb). We left out carbocene because a recent theoretical study of $[C(Cp)_2]$ and $[Si(Cp)_2]$ by Schoeller et al.[61] showed that carbocene prefers a classical dicyclopentadienylcarbene structure, and thus, a discussion in terms of a donor – acceptor metallocene complex is not appropriate. The heavier analogues $[Si(Cp)_2] - [Pb(Cp)_2]$ have been studied before theoretically,[61–63] but the bond energies and heats of formation have not been reported yet.[64] A very recent DFT study about $[Si(Cp)_2] - [Pb(Cp)_2]$ by Smith and Hanusa[63] focussed on the equilibrium geometries and electronic structure of the molecules.

We optimized the geometries of the molecules $[Si(Cp)_2] - [Pb(Cp)_2]$ first with enforced D_{5d} symmetry. The D_{5d} forms are second-order saddle points ($i = 2$). Geometry optimization with less symmetry constraints gave energy minima, which have a bent sandwich structure with C_2 symmetry for $[Si(Cp)]_2$, C_s symmetry for $[Ge(Cp)_2]$ and $[Sn(Cp)_2]$, and C_1 symmetry for $[Pb(Cp)_2]$ (Table 1). The same energy minima were found by Smith and Hanusa, except that they report a C_s form as energy minimum for $[Pb(Cp)_2]$.[63] The energy difference between the C_s and C_1 form is very small (< 0.01 kcal mol^{-1}), and thus, it is not significant. The calculated geometries are in good agreement with experimental values, which have been reported for $[Ge(Cp)_2]$, $[Sn(Cp)_2]$, and $[Pb(Cp)_2]$. For germanocene, the measured Ge–X distance is 2.23 Å, and the bending angle β(X–Ge–X′) is 152°.[65] The calculated values are Ge–X = 2.282 Å and β(X–Ge–X′) = 159.0°. The X-ray structure analysis of stannocene gave two crystallographically independent molecules, which have Sn–X distances between 2.37 – 2.45 Å and bending angles β(X–Sn–X′) of 144 and 148°.[66] The calculated data in Table 1 are Sn–X = 2.490 Å and β(X–Sn–X′) = 151.6°. The experimental values for plumbocene are Pb–X = 2.55 Å and β(X–Pb–X′) = 135 ± 15°.[11a] The calculations give a larger bending angle β(X–Pb–X′) = 156.3°, while the distance Pb–X = 2.586 Å concurs with experimental values.

The calculations predict that the bond energies of the Group 14 metallocenes $[E(Cp)_2]$ have the trend Si > Ge > Sn > Pb, but the differences between the calculated D_e values are not very big. The comparison of the Group 14 sandwich complexes with the alkaline-earth species $[Mg(Cp)_2] - [Ba(Cp)_2]$ shows interesting differences between the trend of the BDE values. The calculated bond energy of $[Si(Cp)_2]$ ($D_e = 130.7$ kcal mol^{-1}) is slightly higher than that of $[Mg(Cp)_2]$ ($D_e = 127.2$ kcal mol^{-1}), but the heavier analogues $[Ge(Cp)_2] - [Pb(Cp)_2]$ have significantly weaker bonds (D_e = 111.3 – 123.2 kcal mol^{-1}) than those of $[Ca(Cp)_2] - [Ba(Cp)_2]$ ($D_e = 154.3 - 166.0$ kcal mol^{-1}). The calculated heats of formation of the Group 14 metallocenes are always strongly positive (Table 1). We want to point out that the heat of formation of silicocene has previously been calculated by Baxter et al.[62a] at a semiempirical level using MNDO.[67] The reported value $\Delta H_f^o([Si(Cp)_2]) = 50.8$ kcal mol^{-1} is much lower than our result $\Delta H_f^o([Si(Cp)_2]) = 99.7$ kcal mol^{-1}. It is possible that the unusual bonding situation of Si in $[Si(Cp)_2]$ may not be correctly described by MNDO, and therefore, the semiempirical value could have a significant error.

Figure 3 shows the trend of the theoretically predicted bond dissociation energies of the half-sandwich and sandwich complexes at CCSD(T)/B. It becomes evident that the D_e values of the four groups of metallocenes change differently when the metal becomes heavier. The Group 1 complexes [Li(Cp)] – [Cs(Cp)] exhibit a significant decrease in bond energy from the first period (Li) to the second period (Na), but then the D_e values remain nearly the same. The Group 2 complexes $[Be(Cp)_2] - [Ba(Cp)_2]$ show also a decrease from the first period (Be) to the second period (Mg), but then the bond energies increase for the next element (Ca) and remain at rather high values for Sr and Ba. The bond energies of the Group 13 complexes [B(Cp)] – [Tl(Cp)] do not

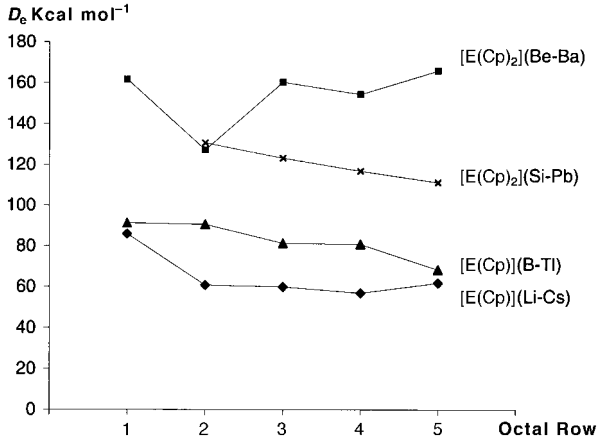

Figure 3. Trend of the theoretically predicted bond dissociation energies D_e at CCSD(T)/B//BP86/A of the sandwich and half-sandwich complexes.

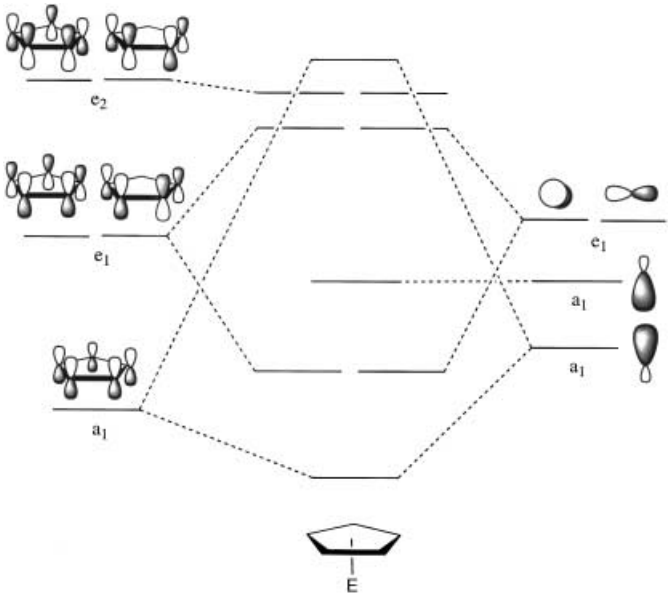

Figure 4. Orbital correlation diagram for half-sandwich complexes [E(Cp)].

change much from the first period (B) to the second (Al), but the D_e values of the next members of the series are smaller. The Group 14 metallocenes show a smooth trend of decreasing bond energies from $[Si(Cp)_2]$ to $[Pb(Cp)_2]$.

Bonding analysis: The bonding model which is generally used for describing the metal–ligand interactions in metallocenes [E(Cp)] and $[E(Cp)_2]$ correlates the atomic orbitals of E^{n+} with the π orbitals of Cp^-. The covalent bonding is then frequently discussed in terms of donor–acceptor interactions between Cp^- and E^+ or E^{2+}, in which electronic charge is donated from the occupied orbitals of Cp^- into vacant orbitals of E^{n+}, and, in the case of transition metals E^{n+}, backdonation takes place between occupied d orbitals of the metal and empty ligand orbitals.[3b, 9b, c, 10–12] The model is very convenient because it considers the bonding between closed-shell species which avoids the problem that arises from assigning three electrons to the degenerate 2π orbital of (D_{5h}) Cp.[68] It should be pointed out that the interactions between Cp^- and E^{n+} must not be confused with the actual driving force of the chemical bonds in metallocenes. The latter arises from the attraction between neutral E and Cp. The conceptually simple donor–acceptor model may legitimately be used, however, for a comparison of the bonding between different metallocenes. We will do this in the following section in a quantitative way by using the results of the energy-partitioning analysis.[15–17]

We begin the discussion with the Group 1 metallocenes [E(Cp)] (E = Li–Cs). Figure 4 shows qualitatively the orbital correlation diagram between the valence orbitals of a main-group element and the π orbitals of Cp^- in (C_{5v}) [E(Cp)]. The six E–Cp bonding valence electrons of the alkali-metal metallocenes occupy the lowest lying a_1 and the degenerate e_1 orbitals. Which of the two orbital interactions is stronger than the other and how important are they compared with the electrostatic attraction? Table 2 gives the results of the energy analysis. The bonding between E^+ and Cp^- has between 80–90% electrostatic character. Thus, the breakdown of the energy contributions supports the classification of the metal–ligand bonding in alkali-metal metallocenes as mainly ionic. As expected, the largest covalent contributions are calculated for [Li(Cp)] ($\Delta E_{orb} = 20.4\%$) and the lowest for [Cs(Cp)] ($\Delta E_{orb} = 10.9\%$). The larger part of the orbital interaction comes always from the e_1 orbital which gives 58–64% of the total ΔE_{orb} value. The a_1 contributions are clearly smaller than the e_1 interactions because the overlap of the a_1 orbitals of E and Cp is not very large. The small contributions by the e_2 term come from the relaxation of the lower lying e_2 σ orbitals of the ligand.

It may be argued that the calculated high percentage of ΔE_{elstat} is caused by the choice of charged fragments rather than neutral species as interacting moieties. Table 2 gives also the calculated atomic partial charges at atom E. The data show that the alkali-metal atoms E carry always a large positive charge, which is close to +1. Thus, the partitioning of [E(Cp)] into $E^+ + Cp^-$ for analyzing the interactions in [E(Cp)] is quite realistic.

Table 2. Energy-decomposition analysis of Group 1 metallocenes [E(Cp)] (E = Li–Cs) at BP86/TZP. The symmetry point group is C_{5v}. All values in kcal mol^{-1}. NBO (natural bond orbital) atomic partial charges q(E) at BP86/A.

Term	Li	Na	K	Rb	Cs
ΔE_{int}	−164.1	−138.0	−120.8	−113.9	−105.9
ΔE_{pauli}	22.6	21.5	27.5	24.1	22.9
ΔE_{elstat}	−148.7 (79.6%)	−138.0 (86.6%)	−128.2 (86.4%)	−121.0 (87.7%)	−114.7 (89.1%)
ΔE_{orb}	−38.1 (20.4%)	−21.4 (13.4%)	−20.1 (13.6%)	−17.0 (12.3%)	−14.1 (10.9%)
A_1	−9.6 (25.2%)	−6.4 (29.9%)	−5.2 (25.7%)	−4.8 (28.4%)	−4.2 (30.0%)
A_2	0.0	0.0	0.0	0.0	0.0
E_1	−24.0 (63.0%)	−12.3 (57.5%)	−13.0 (64.4%)	−10.5 (62.1%)	−8.5 (60.7%)
E_2	−4.5 (11.8%)	−2.7 (12.6%)	−2.0 (9.9%)	−1.6 (9.5%)	−1.3 (9.3%)
q(E)	+0.90	+0.91	+0.91	+0.94	+0.93

0947-6539/02/0820-4700 $ 20.00+.50/0 *Chem. Eur. J.* **2002**, *8*, No. 20

We want to mention two other important points when the effect of charges on ΔE_{elstat} and ΔE_{orb} is considered. Our recent energy analysis of the chemical bonding in isoelectronic metal hexacarbonyls $[TM(CO)_6^q]$ ($TM^q = Hf^{2-}$, Ta^-, W, Re^+, Os^{2+}, Ir^{3+}) has shown that the bonding between the highest charged metals Hf^{2-} and Ir^{3+} and the ligand cage $(CO)_6$ has the lowest degree of electrostatic bonding and the highest degree of covalent bonding.[14a] The counterintuitive result could be explained by the influence of the atomic charge on the energy level of the orbitals. A positive charge lowers the orbital energy levels, which enhances the acceptor strength, while a negative charge raises the orbital levels, which enhances the donor strength. Thus, atomic charges may also strongly enhance the covalent bonding through changing the energy levels of the interacting orbitals. The second point concerns the change in the hybridization which occurs in the fragment orbitals when they relax in the final step of the energy analysis. This leads to an energy decrease of the occupied orbitals even when there is no orbital with the same symmetry in the other fragment because the electrostatic forces change the charge distribution in the fragments. In metallocenes, the relaxation effect of the metal cations should be stronger for the π electrons of the Cp^- ligand than for the σ electrons.

Next we discuss the chemical bonding in the alkaline-earth metallocenes $[E(Cp)_2]$ (E = Be – Ba). The qualitative orbital correlation diagrams between the valence orbitals of a main-group element and the π orbitals of $(Cp^-)_2$ in $[E(Cp)_2]$ complexes with parallel (D_{5d}) and bent (C_{2v}) structures are shown in Figure 5. The orbital diagram for main-group metallocenes is usually given without the d orbitals because they are considered unimportant for the covalent bonding.[11, 12] For reasons which are given below we include the vacant d orbitals of E in Figure 5.

We first discuss the D_{5d} structures. The Group 2 complexes $[E(Cp)_2]$ have 12 valence electrons for $E{-}Cp_2$ bonding which occupy the $1a_{1g}$, $1a_{2u}$, $1e_{1u}$, and $1e_{1g}$ orbitals. Electron donation from the occupied ligand orbitals of $(Cp^-)_2$ into the vacant AOs of E^{2+} takes place via $(1a_{1g}) \rightarrow s(E^{2+})$, $(1a_{2u}) \rightarrow p_z(E^{2+})$, and $(1e_{1u}) \rightarrow p_{x,y}(E^{2+})$, in which z is the bonding axis. There is no valence s or p orbital which has e_{1g} symmetry, and thus, the highest occupied e_{1g} orbital of the ligand should not significantly contribute to the covalent bonding. The only AOs of E which have e_{1g} symmetry are the d_{xz} and d_{yz} orbitals. The covalent bonding in transition-metal (TM) metallocenes may have significant contributions from $(Cp_2^-)e_{1g} \rightarrow d(TM^{2+})$ donation because the d AOs of transition metals are valence orbitals. A recent energy analysis of ferrocene showed that 64.7 % of the covalent bonding comes from $(Cp_2^-)e_{1g} \rightarrow d(Fe^{2+})$ donation.[10a]

Table 3 gives the results of the energy-partitioning analysis of the alkaline-earth metallocenes with D_{5d} symmetry. The attractive interactions between E^{2+} and $(Cp^-)_2$ have more electrostatic than covalent character, but the covalent contributions are larger than in the alkali-metal metallocenes [E(Cp)]. The covalent bonding in beryllocene is 41 % of the total attraction which means that the nature of the metal–ligand interactions in $[Be(Cp)_2]$ has a significantly covalent character. The contributions of the ΔE_{orb} term in the heavier analogues $[Mg(Cp)_2]$ – $[Ba(Cp)_2]$ are only between 17 – 28 %

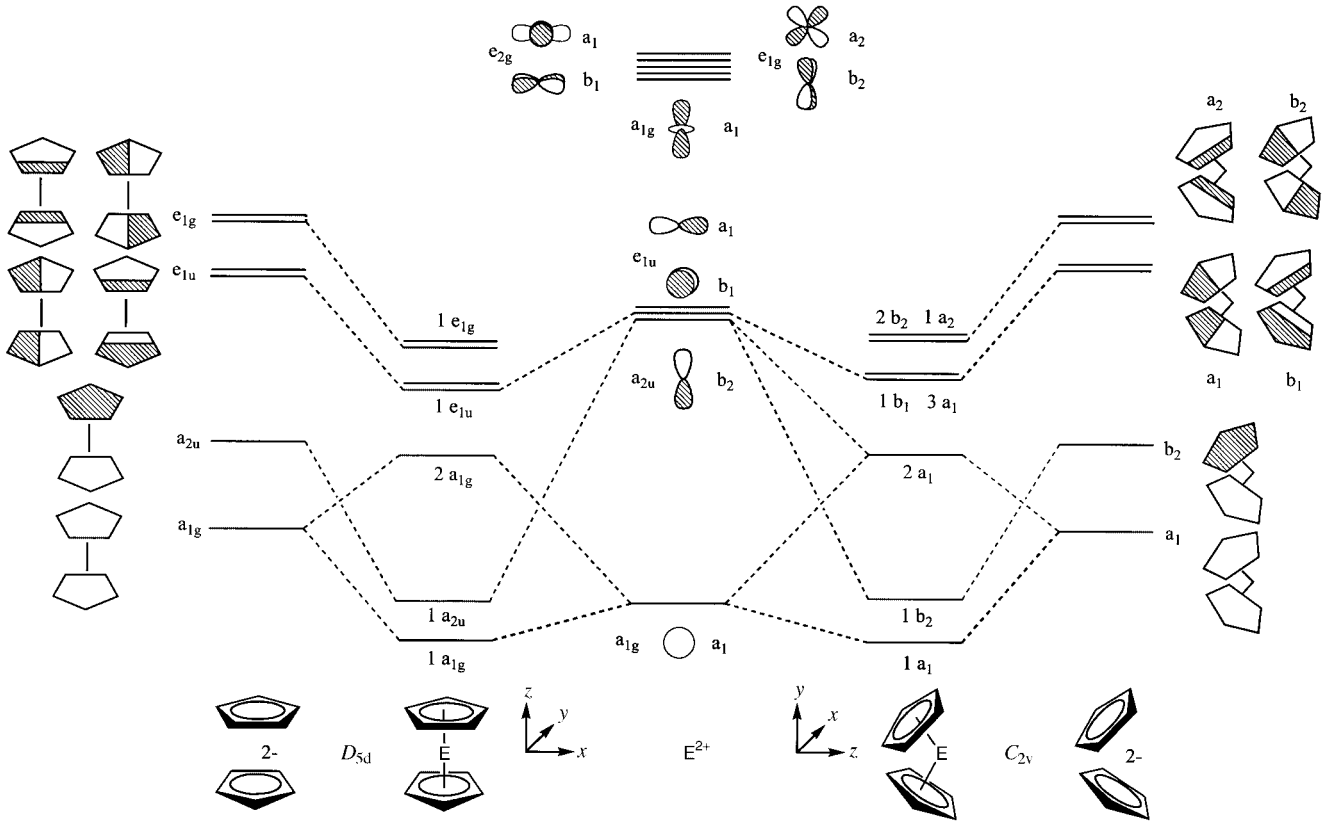

Figure 5. Orbital correlation diagram for sandwich complexes $[E(Cp)_2]$ that includes the d orbitals of the main-group elements.

Table 3. Energy-decomposition analysis of Group 2 metallocenes $[E(Cp)_2]$ (E = Be – Ba) and $[Zn(Cp)_2]$ at BP86/TZP. The symmetry point group is D_{5d}. All values in kcal mol^{-1}. NBO atomic partial charges q(E) at BP86/A.

Term	Be	Mg	Ca	Sr	Ba	Zn
ΔE_{int}	– 780.9	– 636.7	– 549.0	– 504.5	– 461.0	– 707.9
ΔE_{pauli}	35.9	52.7	73.6	66.5	62.2	85.5
ΔE_{elstat}	– 483.2 (59.2 %)	– 493.6 (71.6 %)	– 477.9 (76.8 %)	– 458.3 (80.3 %)	– 437.0 (83.5 %)	– 533.6 (67.3 %)
ΔE_{orb}	– 333.6 (40.8 %)	– 195.8 (28.4 %)	– 144.7 (23.2 %)	– 112.7 (19.7 %)	– 86.2 (16.5 %)	– 259.8 (32.7 %)
A_{1g}	– 58.6 (17.6 %)	– 38.9 (19.9 %)	– 21.5 (14.9 %)	– 18.2 (16.1 %)	– 13.8 (16.0 %)	– 80.6 (31.0 %)
A_{2g}	0.0	0.0	0.0	0.0	0.0	0.0
E_{1g}	– 53.5 (16.0 %)	– 47.6 (24.3 %)	– 63.0 (43.5 %)	– 45.5 (40.4 %)	– 32.0 (37.1 %)	– 39.1 (15.0 %)
E_{2g}	– 15.8 (4.7 %)	– 12.5 (6.4 %)	– 9.1 (6.3 %)	– 7.1 (6.3 %)	– 5.5 (6.4 %)	– 15.1 (5.8 %)
A_{1u}	0.0	0.0	0.0	0.0	0.0	0.0
A_{2u}	– 58.9 (17.6 %)	– 26.6 (13.6 %)	– 13.0 (9.0 %)	– 10.0 (8.9 %)	– 7.9 (9.2 %)	– 35.5 (13.7 %)
E_{1u}	– 132.8 (39.8 %)	– 59.0 (30.1 %)	– 29.6 (20.5 %)	– 24.7 (21.9 %)	– 21.2 (24.6 %)	– 78.4 (30.2 %)
E_{2u}	– 14.1 (4.2 %)	– 11.3 (5.8 %)	– 8.5 (5.9 %)	– 7.2 (6.4 %)	– 5.9 (6.8 %)	– 11.2 (4.3 %)
q(E)	+ 1.68	+ 1.74	+ 1.72	+ 1.77	+ 1.77	+ 1.60

of the total bonding. The positive partial charges at E are between + 1.68 (Be) and + 1.77 (Ba) which means that the partitioning into $E^{2+} + (Cp^-)_2$ is reasonable. Note that the small differences between the positive charge of Be (+ 1.68) and Mg (+ 1.74) do not indicate the substantial difference in covalent bonding between beryllocene and magnesocene.

The breakdown of the ΔE_{orb} term into contributions by the different orbitals shows that, in beryllocene, the strongest interaction comes from the e_{1u} orbitals (39.8 %) followed by the a_{1g} and a_{2u} orbitals (17.6 % each). The small contributions by the e_{2g} (4.7 %) and e_{2u} (4.2 %) orbitals come from the relaxation of ligand σ orbitals through the electrostatic effect of Be^{2+} and by mixing of the $d(e_{2g})$ AOs of the metal with those of the former. There is a somewhat stronger contribution by the e_{1g} orbitals (16.0 %) which arises from the relaxation of the ligand π HOMO and some mixing with the $d(e_{1g})$ polarization function of beryllium. We want to point out that the $d(e_{1g})$ functions of Be have a perfect shape for overlapping with the e_{1g} HOMO of $(Cp^-)_2$.

The change of the orbital contributions of the different alkaline-earth elements to the ΔE_{orb} term is very interesting. Table 3 shows that the stabilization through the e_{1g} orbitals increases relative to the other orbitals when the atom E becomes heavier. In $[Ca(Cp)_2]$, $[Sr(Cp)_2]$, and $[Ba(Cp)_2]$, the contribution of the e_{1g} orbitals becomes the largest component of the ΔE_{orb} term. It is interesting to note that the bonding contribution of the latter orbitals, which involve the metal d AOs, becomes larger than the contributions by the e_{1u}, a_{1g}, and a_{2u} orbitals, which arise from the covalent bonding through the s and p orbitals of atom E. A similar finding was recently reported by Bridgeman.[69] The Mulliken population analysis at the DFT level revealed that the greater π bonding in $[Ca(Cp)_2]$ and $[Sr(Cp)_2]$ was influenced by metal d orbitals, while the d orbital population of Mg in $[Mg(Cp)_2]$ is negligible.[69] We want to point out, however, that the contribution of covalent interactions in $[Ca(Cp)_2]$–$[Ba(Cp)_2]$ is only between 17 – 23 % of the total bonding. Although the *relative* contribution of the e_{1g} orbitals to the ΔE_{orb} term increases from $[Be(Cp)_2]$ to $[Ca(Cp)_2]$, the *absolute* values do not change very much (Table 3). Therefore we do not think that it is justified to classify these molecules as examples, in which the d orbitals become true valence orbitals of heavier main-group elements. Rather they mainly play a role as polarization functions, which are important for the relaxation of the e_{1g} ligand orbitals. However, the orbital correlation diagram shown in Figure 5 would not be sufficient to describe the covalent bonding in alkaline-earth metallocenes without showing the d orbitals, which become more important than the s and p orbitals of atom E.

Table 3 gives also the results of the bonding analysis of zincocene. The data are very interesting because the comparison of the calculated values of $[Zn(Cp)_2]$ with those of the alkaline-earth metallocenes and with ferrocene[10] gives information about the question as to whether Zn behaves more as a transition-metal or as a main-group element. The results show that the bonding in zincocene is similar to the bonding in magnesocene. The attractive interactions between Zn^{2+} and $(Cp^-)_2$ have a higher electrostatic (67 %) than covalent (33 %) character. The electrostatic and covalent interactions in ferrocene have about the same strength.[10] The contributions of the e_{1g} orbitals in $[Zn(Cp)_2]$ are only 15 % of the ΔE_{orb} term because Zn has a filled d shell, and thus, there are no $d(e_{1g})$ acceptor orbitals in zincocene. The most important orbital interactions in $[Zn(Cp)_2]$ come from the a_{1g} and e_{1u} orbitals which arise from the donation of the $(Cp^-)_2$ ligand orbitals into the empty s and p valence orbitals of Zn (Figure 5).

Are the results of the energy analysis of the D_{5d} forms of $[Be(Cp)_2]$, $[Sr(Cp)_2]$, and $[Ba(Cp)_2]$ meaningful when the equilibrium structure of $[Be(Cp)_2]$ has a slipped sandwich geometry, and $[Sr(Cp)_2]$ and $[Ba(Cp)_2]$ are predicted to have bent gometries? We carried out bond energy analyses at BP/TZP by using the energy minima predicted at BP86/A. Although the energy differences between the D_{5d} forms are very small, it is conceivable that there might be significant changes in the components of the interaction energy. The calculations showed that this is not the case. The calculated values of ΔE_{elstat}, ΔE_{Pauli}, and ΔE_{orb} of the (BP86/A) equilibrium geometries were very similar to the data, which are shown in Table 3. The different orbital contributions cannot be compared because the symmetry of the structures is not the same. In order to see if the significant contribution of the metal d orbitals in the heavier alkaline-earth metallocenes is only found in the D_{5d} forms, we calculated bent structures of $[Sr(Cp)_2]$ and $[Ba(Cp)_2]$, in which the Cp rings are rotated and the molecules have C_{2v} symmetry. The energy difference between the C_{2v} structures and the bent equilibrium forms of $[Sr(Cp)_2]$ (C_1) and $[Ba(Cp)_2]$ (C_s) is very small (< 0.1 kcal mol^{-1}). The advantage of the C_{2v} forms is that the orbital terms indicate the contributions, which come from the metal d orbitals. Figure 5 shows that, in the bent C_{2v} structure, the p orbitals of E have a_1, b_1, and b_2 symmetry, and the s orbital has a_1 symmetry. There is no valence AO of E which

0947-6539/02/0820-4702 $ 20.00+.50/0 *Chem. Eur. J.* **2002**, *8*, No. 20

has a_2 symmetry. The HOMO of $(Cp^-)_2$ which has e_{1g} symmetry in the D_{5d} form splits in the C_{2v} form into two components, which have a_2 and b_2 symmetry. Thus, the size of the a_2 contribution to ΔE_{orb} in the C_{2v} form is a probe for the d(E) participation in the orbital interactions.

The results of the energy analysis of the C_{2v} forms of $[Sr(Cp)_2]$ and $[Ba(Cp)_2]$ are given in Table 4. A comparison of the calculated energy contributions in the D_{5d} (Table 3) and C_{2v} (Table 4) forms of $[Sr(Cp)_2]$ and $[Ba(Cp)_2]$ shows that the absolute values of ΔE_{elstat}, ΔE_{Pauli}, and ΔE_{orb} in the bent structures are higher than in the former species. The data of the attractive interactions suggest that the bonding in the C_{2v} form has a slightly higher electrostatic character than in the D_{5d} form, but the difference is not very big. The breakdown of the covalent term into different symmetry contributions shows that the a_2 orbitals are as important as the a_1, b_1, and b_2 orbitals. Thus, the metal d functions are also important in the bent forms of $[Sr(Cp)_2]$ and $[Ba(Cp)_2]$.

Table 4. Energy-decomposition analysis of Group 2 metallocenes $[E(Cp)_2]$ (E = Sr, Ba) at BP86/TZP//BP86/A. The symmetry point group is C_{2v}. All values in kcal mol^{-1}. NBO atomic partial charges q(E) at BP86/A.[a]

Term	Sr	Ba
ΔE_{int}	−505.7	−461.3
ΔE_{pauli}	79.8	88.1
ΔE_{elstat}	−466.9 (79.7%)	−452.8 (82.4%)
ΔE_{orb}	−118.6 (20.3%)	−96.6 (17.6%)
A_1	−35.9 (30.3%)	−30.8 (31.9%)
A_2	−27.9 (23.5%)	−20.8 (21.5%)
B_1	−16.9 (14.2%)	−15.3 (15.8%)
B_2	−37.9 (32.0%)	−29.8 (30.8%)
q(E)	+1.77	+1.74

[a] The partial charges q(E) have been calculated for the bent equilibrium structures.

Next we consider the Group 13 half-sandwich complexes [E(Cp)] (E = B–Tl). The results of the bonding analysis are shown in Table 5. The metal–ligand interactions in the complexes have a higher covalent character than in the Group 1 metallocenes (Table 2). The covalent and electrostatic contributions to the B^+–Cp^- interactions have nearly the same strength (Table 5). Note that the atomic partial charge at boron (+0.18) indicates that the formal electron donation from Cp^- to B^+ is very large. We remind the reader that the choice of ionic fragments as interacting moieties does not necessarily mean that the electrostatic contributions to the bonding are calculated as being too high. The covalent bonding decreases from [Al(Cp)] (35%) to [Tl(Cp)] (28%), which is still higher than in [Li(Cp)] (20%, Table 2). The partial charges at the heavier atoms E do not change very much from Al (+0.61) to Tl (+0.62). The contributions of the a_1 orbitals are significantly higher in the Group 13 complexes (37–44%) than in the Group 1 [E(Cp)] molecules (25–30%). This can be explained by the energy decrease of the acceptor orbitals in B^+–Tl^+ compared with those of Li^+–Cs^+. The energy of the sp-hybridized a_1 orbital is decreased more than in the $p(e_1)$ AOs.

Table 5. Energy-decomposition analysis of Group 13 metallocenes [E(Cp)] (E = B–Tl) at BP86/TZP. The symmetry point group is C_{5v}. All values in kcal mol^{-1}. NBO atomic partial charges q(E) at BP86/A.

Term	B	Al	Ga	In	Tl
ΔE_{int}	−256.0	−188.4	−181.2	−164.6	−155.0
ΔE_{pauli}	202.2	118.1	97.1	81.6	67.2
ΔE_{elstat}	−226.1 (49.3%)	−197.8 (64.6%)	−183.5 (65.9%)	−172.3 (70.0%)	−160.0 (72.0%)
ΔE_{orb}	−232.1 (50.7%)	−108.6 (35.4%)	−94.8 (34.1%)	−73.9 (30.0%)	−62.2 (28.0%)
A_1	−93.9 (40.4%)	−47.9 (44.1%)	−38.4 (40.5%)	−29.7 (40.2%)	−22.7 (36.5%)
A_2	0.0	0.0	0.0	0.0	0.0
E_1	−130.1 (56.1%)	−55.2 (50.8%)	−51.9 (54.8%)	−40.3 (54.5%)	−36.3 (58.4%)
E_2	−8.10 (3.5%)	−5.6 (5.1%)	−4.5 (4.7%)	−3.9 (5.3%)	−3.2 (5.1%)
q(E)	+0.18	+0.61	+0.57	+0.63	+0.62

We finally discuss the bonding analysis of the Group 14 metallocenes $[E(Cp)_2]$ (E = Si–Pb). The results of the D_{5d} structures are shown in Table 6. It becomes evident that the covalent contributions to the E^{2+}–Cp^-_2 interactions are larger than in the Group 2 metallocenes (Table 3), but the ΔE_{elstat} term is still significantly bigger than the ΔE_{orb} term. Note that the ratio of covalent to electrostatic bonding in $[Si(Cp)_2]$–$[Pb(Cp)_2]$ is nearly the same as in [Al(Cp)]–[Tl(Cp)] (Table 5) for elements of the same period. The largest contribution to the covalent bonding in the Group 14 sandwich complexes comes from the e_{1u} orbitals, which contribute 52–55% of the total orbital interactions (Table 6). The e_{1u} orbital term comes from the donation of the occupied ligand orbitals into the vacant $p(\pi)$ AOs of E^{2+} (Figure 5). The relative contributions of the orbitals having different symmetry do not change very much from $[Si(Cp)_2]$ to $[Pb(Cp)_2]$. We want to point out that the e_{1g} orbitals have a rather small weight for ΔE_{orb} even for the largest element Pb. This means that the d functions of the Group 14 elements are not very important for the covalent bonding. This is in agreement with the standard bonding model of main-group metallocenes.[11, 12] The atomic partial charges increase from Si (+0.80) to Pb (+0.99), but they

Table 6. Energy-decomposition analysis of Group 14 metallocenes $[E(Cp)_2]$ (E = Si, Ge, Sn, Pb) at BP86/TZP. The symmetry point group is D_{5d}. All values in kcal mol^{-1}. NBO atomic partial charges q(E) at BP86/A.

Term	Si	Ge	Sn	Pb
ΔE_{int}	−685.4	−661.4	−601.4	−577.2
ΔE_{pauli}	120.4	108.7	101.6	91.3
ΔE_{elstat}	−506.7 (62.9%)	−501.3 (65.1%)	−490.0 (69.7%)	−480.2 (71.8%)
ΔE_{orb}	−299.1 (37.1%)	−268.7 (34.9%)	−213.0 (30.3%)	−188.3 (28.2%)
A_{1g}	−16.6 (5.6%)	−13.2 (4.9%)	−12.2 (5.7%)	−10.3 (5.5%)
A_{2g}	0.0	0.0	0.0	0.0
E_{1g}	−48.9 (16.3%)	−37.7 (14.0%)	−28.9 (13.6%)	−24.9 (13.2%)
E_{2g}	−9.7 (3.2%)	−9.0 (3.3%)	−7.8 (3.6%)	−7.3 (3.9%)
A_{1u}	0.0	0.0	0.0	0.0
A_{2u}	−58.7 (19.6%)	−54.2 (20.2%)	−41.5 (19.5%)	−36.3 (19.3%)
E_{1u}	−156.4 (52.3%)	−146.5 (54.5%)	−115.2 (54.1%)	−102.7 (54.5%)
E_{2u}	−8.8 (2.9%)	−8.2 (3.1%)	−7.5 (3.5%)	−6.8 (3.6%)
q(E)	+0.80	+0.86	+0.98	+0.99

  0947-6539/02/0820-4703 $ 20.00+.50/0

Table 7. Energy-decomposition analysis of Group 14 metallocenes $[E(Cp)_2]$ (E = Si, Ge, Sn, Pb) at BP86/TZP. The symmetry point group is C_{2v}. All values in kcal mol^{-1}. NBO atomic partial charges q(E) at BP86/A.[a]

Term	Si	Ge	Sn	Pb
ΔE_{int}	−690.5	−663.1	−603.9	−577.8
ΔE_{pauli}	144.8	118.9	109.8	93.8
ΔE_{elstat}	−511.6 (61.2%)	−504.1 (64.5%)	−492.5 (69.0%)	−481.0 (71.6%)
ΔE_{orb}	−323.7 (38.8%)	−278.0 (35.5%)	−221.1 (31.0%)	−190.6 (28.4%)
A_1	−117.4 (36.3%)	−97.9 (35.2%)	−79.6 (36.0%)	−66.8 (35.0%)
A_2	−30.1 (9.3%)	−23.4 (8.4%)	−18.8 (8.5%)	−16.1 (8.4%)
B_1	−85.4 (26.4%)	−78.9 (28.4%)	−62.6 (28.3%)	−55.4 (29.1%)
B_2	−90.8 (28.1%)	−77.9 (28.0%)	−60.1 (27.2%)	−52.3 (27.4%)
q(E)	+0.88	+0.89	+1.01	+1.00

[a] The partial charges q(E) have been calculated for the bent equilibrium structures.

are significantly less positive than in the alkaline-earth metallocenes.

Table 7 gives the results of the energy analysis for the bent structures of $[Si(Cp)_2]-[Pb(Cp)_2]$ with C_{2v} symmetry. Unlike the alkaline-earth metallocenes $[Sr(Cp)_2]$ and $[Ba(Cp)_2]$, the covalent contributions are a little stronger in the bent forms than in the D_{5d} structures. The degenerate e_{1u} orbital splits into a_1 and b_1 (Figure 5). Table 7 shows that the sum of the orbital contributions $a_1 + b_1$ provides >60% of the ΔE_{orb} term. Thus, the orbital correlation diagram, which is shown in Figure 5, and the data, which are given in Table 6, provide a reasonable bonding model for the metal–ligand interactions in $[Si(Cp)_2]-[Pb(Cp)_2]$.

Discussion

We want to use the results of the bonding analysis in order to address the question why some metallocenes $[E(Cp)_2]$ have a bent rather than a parallel structure which has been the topic of numerous investigations.[11, 12, 44, 54] Several explanations have been given for the finding that some molecules have bending angles $\beta(X-E-X') < 180^\circ$. The theoretical models that have been suggested to explain the geometries of molecules which exhibit "non-VSEPR" (valence shell electron pair repulsion) structures have recently been discussed in a comprehensive review by Kaupp.[54] We want to point out that, because the energy differences between the linear and bent structures of $[E(Cp)_2]$ are very small, one should be cautious about specifying a particular force, which may be responsible for the bending. The equilibrium geometries of the molecules are the results of all interactions of the involved particles. The desire to find a simple explanation for an interesting observation shall not be an excuse for inappropriate approximations.

Previous theoretical studies led us to the conclusion that the deviation from conventional VSEPR structures correlates with more covalent bonding.[54] This means that metallocenes with more covalent E–Cp bonding should show a stronger tendency towards bent structures. Our calculations show that the covalent contributions to the metal–ligand bonding in $[E(Cp)_2]$ decrease when E is a heavier element. On the other hand, the ligand–ligand repulsion in the sandwich complexes of the lighter atoms E is also stronger because the E–Cp bond lengths are shorter, and therefore, the two factors may compensate each other. However, if covalently bonded metallocenes indeed prefer bent structures, then the bonding analysis should give a higher degree of covalent $E^{2+}-Cp^{-}{}_2$ interactions. Table 8 gives the contributions of ΔE_{elstat}, ΔE_{Pauli}, and ΔE_{orb} to the (bent) equilibrium structures of $[E(Cp)_2]$ (E = Sr, Ba, Si, Ge, Sn, Pb, Zn).

A comparison of the calculated values given in Table 8 with the data for the D_{5d} structures (Tables 3 and 6) shows that the absolute values of the energy terms in the bent forms are always larger than those in the linear structures. The ΔE_{Pauli} term, which gives the strength of the repulsive forces, indicates that as expected the repulsion between the Cp rings in the former structures is larger than in the latter species. This is compensated for in the equilibrium forms by the attractive interactions ΔE_{elstat} and ΔE_{orb}. The calculations show that the contributions of the orbital term play a greater role in the bent form than in the linear form. Thus, the driving forces for bending are indeed the covalent metal–ligand interactions as suggested previously.[54]

It is difficult to specify a particular orbital interaction which is responsible for the increase in the covalent interactions in the bent forms, even when the C_{2v} structures are taken as models for the bent equilibrium structures. The results in Tables 4 and 7 show that the energy terms in the C_{2v} structures and in the equilibrium forms are very similar in size. It has been suggested that the $2a_{1g}$ MO of the D_{5d} form which correlates with the $2a_1$ MO of the C_{2v} form (Figure 5)[70] becomes stabilized due to incorporation of the $p(a_1)$ AO of E. The entries in Tables 4 and 7 show that the a_1 orbitals are indeed the strongest contributor to the ΔE_{orb} term except for in $[Sr(Cp)_2]$, for which the a_1 value is slightly less than for the b_2 data. However, the a_1 orbitals in the C_{2v} form correlate also with one component of the degenerate e_{1u} orbital of the D_{5d} form (Figure 5). Thus, it is not possible to say that one particular orbital is the driving force of the stronger covalent interactions in the bent form.

Table 8. Energy-decomposition analysis of the $[E(Cp)_2]$ at the bent equilibrium geometry (E = Sr, Ba, Si, Ge, Sn, Pb, Zn) at BP86/TZP. All values in kcal mol^{-1}.

Term	Sr (C_1)[a]	Ba (C_s)[a]	Si (C_2)[b]	Ge (C_s)[b]	Sn (C_s)[b]	Pb (C_1)[b]	Zn (C_s)[b]
ΔE_{int}	−505.6	−461.4	−691.9	−663.2	−604.0	−578.0	−720.0
ΔE_{pauli}	79.6	87.6	153.1	119.4	110.1	94.5	113.3
ΔE_{elstat}	−466.8 (79.7%)	−452.7 (82.4%)	−513.2 (60.7%)	−504.0 (64.4%)	−492.5 (69.0%)	−481.6 (71.7%)	−553.1 (66.4%)
ΔE_{orb}	−118.4 (20.3%)	−96.3 (17.6%)	−331.8 (39.3%)	−278.7 (35.6%)	−221.6 (31.0%)	−190.8 (28.3%)	−280.2 (33.6%)

[a] BP86/TZP//BP86/A. [b] BP86/TZP//BP86/TZP.

0947-6539/02/0820-4704 $ 20.00+.50/0 *Chem. Eur. J.* **2002**, *8*, No. 20

Conclusion

The results of this work can be summarized as follows.

1) The equilibrium geometries of the Group 1 and Group 13 metallocenes [E(Cp)] (E = Li–Cs, B–Tl) have C_{5v} symmetry. The Group 2 sandwich complexes [E(Cp)$_2$] have fluxional structures. The energetically lowest lying geometries of [Mg(Cp)$_2$] and [Ca(Cp)$_2$] have D_{5d} symmetry, while the most stable structures of [Sr(Cp)$_2$] and [Ba(Cp)$_2$] are bent. [Be(Cp)$_2$] has a slipped sandwich structure. A slipped sandwich structure is also calculated for [Zn(Cp)$_2$]. The Group 14 metallocenes [E(Cp)$_2$] (E = Si–Pb) have bent equilibrium geometries, which are only slightly lower in energy than the D_{5d} structures.
2) The trends of the E–Cp$_n$ bond energies are quite different for the elements E of Groups 1, 2, 13, and 14. The calculated bond dissociation energies of the alkali-metal metallocenes change little from [Na(Cp)] (D_e = 60.8 kcal mol^{-1}) to [Cs(Cp)] (D_e = 61.8 kcal mol^{-1}), while the value for [Li(Cp)] (D_e = 86.0 kcal mol^{-1}) is clearly higher. Magnesocene has clearly the weakest metal–ligand bonds among the Group 2 complexes (D_e = 127.2 kcal mol^{-1}), while the values for [Be(Cp)$_2$] (D_e = 161.7 kcal mol^{-1}), [Ca(Cp)$_2$] (D_e = 160.3 kcal mol^{-1}), [Sr(Cp)$_2$] (D_e = 154.3 kcal mol^{-1}), and [Ba(Cp)$_2$] (D_e = 166.0 kcal mol^{-1}) are higher and do not vary very much. The calculated bond energy of zincocene (D_e = 74.9 kcal mol^{-1}) is much lower than those of the main-group metallocenes [E(Cp)$_2$]. The bond energies of the Group 13 half-sandwich complexes exhibit the trend: [B(Cp)] (D_e = 91.3 kcal mol^{-1}) ≈ [Al(Cp)] (D_e = 90.7 kcal mol^{-1}) > [Ga(Cp)] (D_e = 81.3 kcal mol^{-1}) ≈ [In(Cp)] (D_e = 80.8 kcal mol^{-1}) > [Tl(Cp)] (D_e = 68.4 kcal mol^{-1}). A smooth trend of decreasing bond energies from [Si(Cp)$_2$] (D_e = 130.7 kcal mol^{-1}) to [Pb(Cp)$_2$] (D_e = 111.3 kcal mol^{-1}) is predicted for the Group 14 complexes. The theoretically predicted heats of formation are positive for all complexes except for [Ca(Cp)$_2$], [Sr(Cp)$_2$], and [Ba(Cp)$_2$], which have ΔH_f^o values ≈0 kcal mol^{-1}.
3) The energy-decomposition analysis of the interactions between E^{n+} and $(Cp^-)_n$ suggests that, in the alkali-metal metallocenes [Li(Cp)]–[Tl(Cp)], the electrostatic contributions are 80–90% of the total attraction. The strongest covalent interactions are found in [Li(Cp)] (20%). The orbital interactions come mainly from the π donation of the e_1 ligand orbital into the vacant p(π) AOs of the metals. The bonding in the heavier alkaline-earth metallocenes is also mainly caused by electrostatic forces which contribute 72% (Mg)–84% (Ba) to the total interaction energy. Beryllocene has a significant covalent contribution to the bonding interaction (41%). The orbital interactions in beryllocene come mainly from the orbitals which have e_{1u} (40%), a_{2u} (18%), and a_{1g} (18%) symmetry, which correlate with the electron donation from the occupied ligand orbitals into the vacant p(π), p(σ), and s AOs of Be. The largest contributions to the ΔE_{orb} term of the heavier complexes [Ca(Cp)$_2$]–[Ba(Cp)$_2$] come from the e_{1g} orbital, which corresponds to the d orbitals of the metals. This is more a relaxation effect of the ligand orbital rather than genuine covalent metal–ligand bonding. The calculated energy terms of the metal–ligand interactions in [Zn(Cp)$_2$] suggest that the bonding situation in zincocene is similar to that in magnesocene. The ratio of electrostatic to covalent bonding in the parallel (D_{5d}) and bent forms of the two molecules is nearly the same. The bent forms of [Zn(Cp)$_2$] and [Mg(Cp)$_2$] have a slightly higher covalent character than in the parallel forms.

The covalent contributions to the bonding in the Group 13 metallocenes are still higher than those in the Group 2 metallocenes. The covalent and electrostatic attractions in boracene have nearly equal strength, while the covalent bonding in the heavier analogues contributes between 28% ([Tl(Cp)]) and 35% ([Al(Cp)]) to the total attraction. The a_1 (σ) orbital interactions contribute 37–44% to the ΔE_{orb} term, while 51–58% comes from the e_1 (π) orbitals. The attractive interactions in the Group 14 sandwich complexes [Si(Cp)$_2$]–[Pb(Cp)$_2$] have between 63–72% electrostatic character. The covalent bonding in the latter species comes mainly (52–55%) from the e_{1u} orbitals. The metal–Cp bonds in the bent forms have a higher covalent character than in the D_{5d} structures.

Acknowledgements

This work was supported by the Deutsche Forschungsgemeinschaft and by the Fonds der Chemischen Industrie. V.M.R. thanks the Secretaría de Estado de Educación y Universidades (MECD-Spain) for support by grant EX-01-09396368V. Excellent service by the Hochschulrechenzentrum of the Philipps-Universität Marburg is gratefully acknowledged. Additional computer time was provided by the HLRS Stuttgart.

[1] T. J. Kealy, P. L. Pauson, *Nature* **1951**, *168*, 1039.
[2] Another paper which reported the synthesis of ferrocene was submitted earlier than reference [1], but it was published later: S. A. Miller, J. A. Tebboth, J. F. Tremaine, *J. Chem. Soc.* **1952**, 633.
[3] a) A special issue dedicated to ferrocene in: *J. Organomet. Chem.* **2001**, *637*; b) C. Elschenbroich, A. Salzer, *Organometallics* 2nd ed., VCH, Weinheim, **1992**, p. 3.
[4] *Metallocenes* (Eds.: A. Togni, R. L. Haltermann), Wiley, New York, **1998**.
[5] *Homogeneous Catalysis with Organometallic Compounds*, *Vols. 1* and *2* (Eds.: B. Cornils, W. A. Herrmann), VCH, Weinheim, **1996**.
[6] E. O. Fischer, W. Pfab, *Z. Naturforsch.* **1952**, *76*, 377.
[7] G. Wilkinson, M. Rosenblum, M. C. Whiting, R. B. Woodward, *J. Am. Chem. Soc.* **1952**, *74*, 2125.
[8] E. M. Shustorovich, E. M. Dyatkina, *Dokl. Akad. Nauk. SSSR* **1959**, *128*, 1234.
[9] a) C. Elschenbroich, A. Salzer, *Organometallics* 2nd ed., VCH, Weinheim, **1992**, p. 320; b) T. A. Albright, J. K. Burdett, M. H. Whangbo, *Orbital Interactions in Chemistry*, Wiley, New York, **1985**, p. 393; c) F. A. Cotton, G. Wilkinson, C. A. Murillo, M. Bochmann, *Advanced Inorganic Chemistry* 6th. ed., Wiley, New York, **1999**, p. 686.
[10] a) M. Lein, J. Frunzke, A. Timoshkin, G. Frenking, *Chem. Eur. J.* **2001**, *7*, 4155; b) J. Frunzke, M. Lein, G. Frenking, *Organometallics* **2002**, *21*, 3351.
[11] a) P. Jutzi, N. Burford, *Chem. Rev.* **1999**, *99*, 969; b) P. Jutzi, N. Burford, *Metallocenes*, *Vol. 1* (Eds.: A. Togni, R. L. Haltermann), Wiley, New York, **1998**, p. 3.
[12] O. Kwon, M. L. McKee in *Computational Organometallic Chemistry* (Ed.: T. R. Cundari), Marcel Dekker, New York, **2001**, p. 397f.

  0947-6539/02/0820-4705 $ 20.00+.50/0

[13] O. Kwon, M. L. McKee in *Computational Organometallic Chemistry* (Ed.: T. R. Cundari), Marcel Dekker, New York, **2001**, p. 403.

[14] a) A. Diefenbach, F. M. Bickelhaupt, G. Frenking, *J. Am. Chem. Soc.* **2000**, *122*, 6449; b) J. Uddin, G. Frenking, *J. Am. Chem. Soc.* **2001**, *123*, 1683; c) Y. Chen, G. Frenking, *J. Chem. Soc. Dalton Trans.* **2001**, 434; d) G. Frenking, K. Wichmann, N. Fröhlich, J. Grobe, W. Golla, D. Le Van, B. Krebs, M. Läge, *Organometallics* **2002**, *21*, 2921.

[15] F. M. Bickelhaupt, E. J. Baerends, *Reviews in Computational Chemistry*, *Vol. 15* (Eds.: K. B. Lipkowitz, D. B. Boyd), Wiley, New York, **2000**, p. 1.

[16] K. Morokuma, *J. Chem. Phys.* **1971**, *55*, 1236.

[17] T. Ziegler, A. Rauk, *Thermochim. Acta* **1977**, *46*, 1.

[18] A. D. Becke, *Phys. Rev. A*: *At. Mol. Opt. Phys.* **1988**, *38*, 3098.

[19] J. P. Perdew, *Phys. Rev. B.*: *Condens. Matter Mater. Phys.* **1986**, *33*, 8822.

[20] a) R. Ditchfield, W. J. Hehre, J. A. Pople, *J. Chem. Phys.* **1971**, *54*, 724; b) W. J. Hehre, R. Ditchfield, J. A. Pople, *J. Chem. Phys.* **1972**, *56*, 2257; c) P. C. Hariharan, J. A. Pople, *Thermochim. Acta* **1973**, *28*, 213; d) F. J. D. Dill, J. A. Pople, *J. Chem. Phys.* **1975**, *62*, 2921; e) M. M. Francl, W. J. Pietro, W. J. Hehre, J. S. Binkley, M. S. Gordon, D. J. Defrees, J. A. Pople, *J. Chem. Phys.* **1982**, *77*, 3654; f) M. S. Gordon, J. S. Binkley, J. A. Pople, W. J. Pietro, W. J. Hehre, *J. Am. Chem. Soc.* **1982**, *104*, 2797.

[21] V. A. Rassolov, M. A. Ratner, J. A. Pople, P. C. Redfern, L. A. Curtiss, *J. Comput. Chem.* **2001**, *22*, 976.

[22] T. Leininger, A. Nicklass, W. Kuechle, H. Stoll, M. Dolg, A. Bergner, *Chem. Phys. Lett.* **1996**, *255*, 274.

[23] M. Kaupp, P. v. R. Schleyer, H. Stoll, H. Preuss, *J. Chem. Phys.* **1991**, *94*, 1360.

[24] a) A. Bergner, M. Dolg, W. Kuechle, H. Stoll, H. Preuss, *Mol. Phys.* **1993**, *80*, 1431; b) W. Kuechle, M. Dolg, H. Stoll, H. Preuss, *Mol. Phys.* **1991**, *74*, 1245.

[25] Gaussian Basis Sets for Molecular Calculations, S. Huzinaga, J. Anzelm, M. Klobukowski, E. Radzio-Andzelm, Y. Sakai, H. Tatewaki, Elsevier, Amsterdam, **1984**.

[26] M. Dolg, U. Wedig, H. Stoll, H. Preuss, *J. Chem. Phys.* **1987**, *86*, 866.

[27] Gaussian 98 (Revision A.7), M. J. Frisch, G. W. Trucks, H. B. Schlegel, G. E. Scuseria, M. A. Robb, J. R. Cheeseman, V. G. Zakrzewski, J. A. Montgomery, Jr., R. E. Stratmann, J. C. Burant, S. Dapprich, J. M. Millam, A. D. Daniels, K. N. Kudin, M. C. Strain, O. Farkas, J. Tomasi, V. Barone, M. Cossi, R. Cammi, B. Mennucci, C. Pomelli, C. Adamo, S. Clifford, J. Ochterski, G. A. Petersson, P. Y. Ayala, Q. Cui, K. Morokuma, D. K. Malick, A. D. Rabuck, K. Raghavachari, J. B. Foresman, J. Cioslowski, J. V. Ortiz, A. G. Baboul, B. B. Stefanov, G. Liu, A. Liashenko, P. Piskorz, I. Komaromi, R. Gomperts, R. L. Martin, D. J. Fox, T. Keith, M. A. Al-Laham, C. Y. Peng, A. Nanayakkara, C. Gonzalez, M. Challacombe, P. M. W. Gill, B. Johnson, W. Chen, M. W. Wong, J. L. Andres, C. Gonzalez, M. Head-Gordon, E. S. Replogle, J. A. Pople, Gaussian, Inc., Pittsburgh, PA, **1998**.

[28] R. J. Bartlett, J. F. Stanton, *Reviews in Computational Chemistry*, *Vol. 5* (Eds.: K. B. Lipkowitz, D. B. Boyd), VCH, New York, **1994**.

[29] a) C. Hampel, K. Peterson, H.-J. Werner, *Chem. Phys. Lett.* **1992**, *190*, 1, and references therein; b) J. D. Watts, J. Gauss, R. J. Bartlett, *J. Chem. Phys.* **1993**, *98*, 8718.

[30] MOLPRO is a package of ab initio programs: MOLPRO, H.-J. Werner, P. J. Knowles, R. D. Amos, A. Bernhardsson, A. Berning, P. Celani, D. L. Cooper, M. J. O. Deegan, A. J. Dobbyn, F. Eckert, C. Hampel, G. Hetzer, T. Korona, R. Lindh, A. W. Lloyd, S. J. McNicholas, F. R. Manby, W. Meyer, M. E. Mura, A. Nicklass, P. Palmieri, R. Pitzer, G. Rauhut, M. Schütz, H. Stoll, A. J. Stone, R. Tarroni, T. Thorsteinsson, Stuttgart, **2001**.

[31] P. J. Knowles, C. Hampel, H.-J. Werner, *J. Chem. Phys.* **1993**, *99*, 5219; Erratum: P. J. Knowles, C. Hampel, H.-J. Werner, *J. Chem. Phys.* **2000**, *112*, 3106.

[32] R. Krishnan, J. S. Binkley, R. Seeger, J. A. Pople, *J. Chem. Phys.* **1980**, *72*, 650.

[33] A. D. McLean, G. S. Chandler, *J. Chem. Phys.* **1980**, *72*, 5639.

[34] a) F. M. Bickelhaupt, E. J. Baerends, *Reviews in Computational Chemistry*, *Vol. 15* (Eds.: K. B. Lipkowitz, D. B. Boyd), Wiley, New York, **2000**, p. 1; b) G. te Velde, F. M. Bickelhaupt, E. J. Baerends, S. J. A. van Gisbergen, C. Fonseca Guerra, J. G. Snijders, T. Ziegler, *J. Comput. Chem.* **2001**, *22*, 931.

[35] a) E. van Lenthe, E. J. Baerends, J. G. Snijders, *J. Chem. Phys.* **1993**, *99*, 4597; b) E. van Lenthe, E. J. Baerends, J. G. Snijders, *J. Chem. Phys.* **1994**, *101*, 9783; c) E. van Lenthe, A. E. Ehlers, E. J. Baerends, *J. Chem. Phys.* **1999**, *110*, 8943; d) E. van Lenthe, J. G. Snijders, E. J. Baerends, *J. Chem. Phys.* **1996**, *105*, 6505; e) E. van Lenthe, R. van Leeuwen, E. J. Baerends, J. G. Snijders, *Int. J. Quantum Chem.* **1996**, *57*, 281.

[36] J. G. Snijders, E. J. Baerends, P. Vernooijs, *At. Data Nucl. Data Tables* **1982**, *26*, 483.

[37] J. Krijn, E. J. Baerends, *Fit Functions in the HFS-Method*, Internal Report (in Dutch), Vrije Universiteit Amsterdam, The Netherlands, **1984**, 1.

[38] The following ΔH_f^o values have been used: $\Delta H_f^o(\mathrm{Li}) = 37.7\ \mathrm{kcal\,mol^{-1}}$; $\Delta H_f^o(\mathrm{Na}) = 25.7\ \mathrm{kcal\,mol^{-1}}$; $\Delta H_f^o(\mathrm{K}) = 21.5\ \mathrm{kcal\,mol^{-1}}$; $\Delta H_f^o(\mathrm{Rb}) = 19.6\ \mathrm{kcal\,mol^{-1}}$; $\Delta H_f^o(\mathrm{Cs}) = 18.5\ \mathrm{kcal\,mol^{-1}}$; $\Delta H_f^o(\mathrm{Be}) = 76.5\ \mathrm{kcal\,mol^{-1}}$; $\Delta H_f^o(\mathrm{Mg}) = 35.0\ \mathrm{kcal\,mol^{-1}}$; $\Delta H_f^o(\mathrm{Ca}) = 42.5\ \mathrm{kcal\,mol^{-1}}$; $\Delta H_f^o(\mathrm{Sr}) = 39.0\ \mathrm{kcal\,mol^{-1}}$; $\Delta H_f^o(\mathrm{Ba}) = 43.0\ \mathrm{kcal\,mol^{-1}}$; $\Delta H_f^o(\mathrm{Zn}) = 31.0\ \mathrm{kcal\,mol^{-1}}$; $\Delta H_f^o(\mathrm{B}) = 133.3\ \mathrm{kcal\,mol^{-1}}$; $\Delta H_f^o(\mathrm{Al}) = 78.8\ \mathrm{kcal\,mol^{-1}}$; $\Delta H_f^o(\mathrm{Ga}) = 64.8\ \mathrm{kcal\,mol^{-1}}$; $\Delta H_f^o(\mathrm{In}) = 58.2\ \mathrm{kcal\,mol^{-1}}$; $\Delta H_f^o(\mathrm{Tl}) = 43.7\ \mathrm{kcal\,mol^{-1}}$; $\Delta H_f^o(\mathrm{Si}) = 106.0\ \mathrm{kcal\,mol^{-1}}$; $\Delta H_f^o(\mathrm{Ge}) = 89.3\ \mathrm{kcal\,mol^{-1}}$; $\Delta H_f^o(\mathrm{Sn}) = 72.2\ \mathrm{kcal\,mol^{-1}}$; $\Delta H_f^o(\mathrm{Pb}) = 46.8\ \mathrm{kcal\,mol^{-1}}$; $\Delta H_f^o(\mathrm{Cp}) = 58.0\ \mathrm{kcal\,mol^{-1}}$. The data were taken from reference [55].

[39] a) E. D. Jemmis, P. v. R. Schleyer, *J. Am. Chem. Soc.* **1982**, *104*, 4781; b) L. Lattman, A. H. Cowley, *Inorg. Chem.* **1984**, *23*, 241; c) K. C. Waterman, A. Streitwieser, Jr., *J. Am. Chem. Soc.* **1984**, *106*, 3138; d) R. Blom, K. Faegri, Jr., T. Midtgaard, *J. Am. Chem. Soc.* **1991**, *113*, 3230; e) M. Bühl, N. J. R. van Eikema Hommes, P. v. R. Schleyer, U. Fleischer, W. Kutzelnigg, *J. Am. Chem. Soc.* **1991**, *113*, 2459; f) M. N. Glukhovtsev, P. v. R. Schleyer, C. Maerker, *J. Phys. Chem.* **1993**, *97*, 8200; g) A. Bérces, T. Ziegler, L. Fan, *J. Phys. Chem.* **1994**, *98*, 1584; h) L. M. Pratt, I. M. Khan, *J. Comput. Chem.* **1995**, *16*, 1067; i) C. Dohmeier, E. Baum, A. Ecker, R. Köppe, H. Schnöckel, *Organometallics* **1996**, *15*, 4702; j) B. Goldfuss, P. v. R. Schleyer, *Organometallics* **1997**, *16*, 1543; k) H. Jiao, P. v. R. Schleyer, Y. Mo, M. A. McAllister, T. T. Tidwell, *J. Am. Chem. Soc.* **1997**, *119*, 7075; l) C. Üffing, R. Köppe, H. Schnöckel, *Organometallics* **1998**, *17*, 3512; m) M. J. Harvey, T. P. Hanusa, *Organometallics* **2000**, *19*, 1556.

[40] S. Harder, M. Lutz, S. J. Obert, *Organometallics* **1999**, *18*, 1808.

[41] a) S. Harder, M. H. Prosenc, *Angew. Chem.* **1996**, *108*, 101; *Angew. Chem. Int. Ed. Engl.* **1996**, *35*, 97; b) R. E. Dinnebier, F. Olbrich, G. M. Bendele, *Acta Crystallogr. Sect. C*: *Cryst. Struct. Commun.* **1997**, *53*, 699.

[42] W. Strohmeier, H. Landsfeld, F. Gernert, *Z. Elektrochem.* **1962**, *66*, 823.

[43] a) E. D. Jemmis, S. Alexandratos, P. v. R. Schleyer, A. Streitwieser, Jr., H. F. Schaefer III, *J. Am. Chem. Soc.* **1978**, *100*, 5695; b) N.-S. Chiu, L. Schäfer, *J. Am. Chem. Soc.* **1978**, *100*, 2604; c) V. T. Aleksanyan, I. I. Greenwald, *THEOCHEM* **1982**, *90*, 35; d) J. Almlöf, K. Faegri, Jr., B. E. R. Schilling, *Chem. Phys. Lett.* **1984**, *106*, 266; e) R. Blom, K. Faegri, Jr., H. V. Volden, *Organometallics* **1990**, *9*, 372; f) M. Kaupp, P. v. R. Schleyer, M. Dolg, H. Stoll, *J. Am. Chem. Soc.* **1992**, *114*, 8202; g) P. Margl, K. Schwarz, P. E. Blöchl, *J. Am. Chem. Soc.* **1994**, *116*, 11177; h) I. Bytheway, P. L. A. Popelier, R. J. Gillespie, *Can. J. Chem.* **1996**, *74*, 1059; i) V. Milman, M.-H. Lee, *J. Phys. Chem.* **1996**, *100*, 6093; j) K. Schwarz, E. Nusterer, P. Margl, P. E. Blöchl, *Int. J. Quant. Chem.* **1997**, *61*, 369; k) L. W. Mire, S. D. Wheeler, E. Wagenseller, D. S. Marynick, *Inorg. Chem.* **1998**, *37*, 3099; l) J. Cioslowski, M. Schimeczek, G. Liu, V. Stoyanov, *J. Chem. Phys.* **2000**, *113*, 9377.

[44] a) T. P. Hanusa, *Polyhedron* **1990**, *9*, 1435; b) T. P. Hanusa, *Chem. Rev.* **1993**, *93*, 1023; c) M. L. Hays, T. P. Hanusa, *Adv. Organomet. Chem.* **1996**, *40*, 117.

[45] C. Elschenbroich, A. Salzer, *Organometallics* 2nd ed., VCH, Weinheim, **1992**, p. 39f.

[46] E. O. Fischer, H. P. Hofmann, *Chem. Ber.* **1959**, *92*, 482.

[47] C. Wong, S. Wang, *Inorg. Nucl. Chem. Lett.* **1975**, *11*, 677.

[48] a) A. Almenningen, O. Bastiansen, A. Haaland, *J. Chem. Phys.* **1964**, *40*, 3434; b) A. Almenningen, A. Haaland, J. Lusztyk, *J. Organomet. Chem.* **1979**, *170*, 271.

[49] K. W. Nugent, J. K. Beattie, T. W. Hambley, M. R. Snow, *Aust. J. Chem.* **1984**, *37*, 1601.

[50] A. Haaland, J. Lusztyk, J. Brunvoll, K. Z. Starowieyscki, *J. Organomet. Chem.* **1975**, *85*, 279.

  0947-6539/02/0820-4706 $ 20.00+.50/0

[51] W. Bünder, E. Weiss, *J. Organomet. Chem.* **1975**, *92*, 1.
[52] a) R. A. Andersen, R. Blom, J. M. Boncella, C. J. Burns, H. V. Volden, *Acta Chem. Scand.* **1987**, *A41*, 24; b) R. A. Andersen, R. Blom, C. J. Burns, H. V. Volden, *J. Chem. Soc. Chem. Commun.* **1987**, 768.
[53] R. A. Williams, T. P. Hanusa, J. C. Huffman, *Organometallics* **1990**, *9*, 1128.
[54] M. Kaupp, *Angew. Chem.* **2001**, *113*, 3642; *Angew. Chem. Int. Ed.* **2001**, *40*, 3534.
[55] S. G. Lias, J. E. Bartmess, J. F. Liebman, J. L. Holmes, R. D. Levin, W. G. Mallard, *J. Phys. Chem. Ref. Data* **1988**, *17*, Suppl. 1.
[56] R. Blom, A. Haaland, J. Weidlein, *J. Chem. Soc. Chem. Commun.* **1985**, 266.
[57] a) V. G. Zakrzewski, J. V. Ortiz, *J. Phys. Chem.* **1994**, *98*, 13198; b) V. G. Zakrzewski, J. V. Ortiz, *Int. J. Quantum Chem.* **1994**, *28*, 23.
[58] a) C. S. Ewig, R. Osman, J. R. Van Wazer, *J. Am. Chem. Soc.* **1978**, *100*, 5017; b) W. J. Pietro, E. S. Blurock, R. T. Hout, Jr., W. J. Hehre, D. J. DeFrees, R. F. Stewart, *Inorg. Chem.* **1981**, *20*, 3650; c) E. Canadell, O. Eisenstein, J. Rubio, *Organometallics* **1984**, *3*, 759; d) R. Alhrichs, M. Ehrig, H. Horn, *Chem. Phys. Lett.* **1991**, *183*, 227; e) D. Loos, H. Schnöckel, J. Gauss, U. Schneider, *Angew. Chem.* **1992**, *104*, 1376; *Angew. Chem. Int. Ed. Engl.* **1992**, *31*, 1362; f) D. R. Armstrong, R. Herbst-Irmer, A. Kuhn, D. Moncrieff, M. A. Paver, C. A. Russell, D. Stalke, A. Steiner, D. S. Wright, *Angew. Chem.* **1993**, *105*, 1807; *Angew. Chem. Int. Ed. Engl.* **1993**, *32*, 1774; g) J. Gauss, U. Schneider, R. Ahlrichs, C. Dohmeier, H. Schnöckel, *J. Am. Chem. Soc.* **1993**, *115*, 2402; h) C. Üffing, A. Ecker, R. Köppe, H. Schnöckel, *Organometallics* **1998**, *17*, 2373; i) P. Pyykkö, M. Straka, T. Tamm, *Phys. Chem. Chem. Phys.* **1999**, *1*, 3441; j) C. L. B. Macdonald, A. H. Cowley, *J. Am. Chem. Soc.* **1999**, *121*, 12113; k) J. Uddin, C. Boehme, G. Frenking, *Organometallics* **2000**, *19*, 571.
[59] A. Haaland, K.-G. Martinsen, S. A. Shlykov, H. V. Volden, C. Dohmeier, H. Schnöckel, *Organometallics*, **1995**, *14*, 3116.
[60] A. Haaland, K.-G. Martinsen, H. V. Volden, D. Loos, H. Schnöckel, *Acta Chem. Scand.* **1994**, *48*, 172.
[61] W. W. Schoeller, O. Friedrich, A. Sundermann, A. Rozhenko, *Organometallics* **1999**, *18*, 2099.
[62] a) S. G. Baxter, A. H. Cowley, J. G. Lasch, M. Lattman, W. P. Sharum, C. A. Stewart, *J. Am. Chem. Soc.* **1982**, *104*, 4064; b) A. Haaland, B. E. R. Schilling, *Acta Chem. Scand.* **1984**, *A38*, 217; c) P. Jutzi, U. Holtmann, D. Kanne, C. Krüger, R. Blom, R. Gleiter, I. Hyla-Krypsin, *Chem. Ber.* **1989**, *122*, 1629; d) T. J. Lee, J. E. Rice, *J. Am. Chem. Soc.* **1989**, *111*, 2011; e) D. R. Armstrong, M. J. Duer, M. G. Davidson, D. Moncrieff, C. A. Russell, C. Stourton, A. Steiner, D. Stalke, D. S. Wright, *Organometallics* **1997**, *16*, 3340; f) D. R. Armstrong, M. A. Beswick, N. L. Cromhout, C. N. Harmer, D. Moncrieff, C. A. Russell, P. R. Raithby, A. Steiner, A. E. H. Wheatley, D. S. Wright, *Organometallics* **1998**, *17*, 3176; g) W. W. Schoeller, O. Friedrich, A. Sundermann, A. Rozhenko, *Organometallics* **1999**, *18*, 2099; h) S. P. Constantine, H. Cox, P. B. Hitchcock, G. A. Lawless, *Organometallics* **2000**, *19*, 317.
[63] J. D. Smith, T. P. Hanusa, *Organometallics* **2001**, *20*, 3056.
[64] The heat of formation of plumbocene has been calculated with the semiempirical method MNDO.[67] The theoretical value $\Delta H_f^\circ([Pb(Cp)_2]) = 134\ kcal\,mol^{-1}$ is much higher than the result which is given here. We do not think that the MNDO value is reliable: M. J. S. Dewar, M. K. Holloway, G. L. Grady, J. J. P. Stewart, *Organometallics* **1985**, *4*, 1973.
[65] M. Grenz, E. Hahn, W. W. du Mont, J. Pickardt, *Angew. Chem.* **1984**, *96*, 69; *Angew. Chem. Int. Ed. Engl.* **1984**, *23*, 61.
[66] J. L. Atwood, W. E. Hunter, A. H. Cowley, R. A. Jones, C. A. Stewart, *J. Chem. Soc. Chem. Commun.* **1981**, 925.
[67] M. J. S. Dewar, W. Thiel, *J. Am. Chem. Soc.* **1977**, *99*, 4899.
[68] A possible solution to the problem might be to use fractional occupation numbers, for which the two components of the degenerate π orbital of Cp receive the same electronic charge. We are currently investigating the possibility of using fractional occupation numbers.
[69] A. J. Bridgeman, *J. Chem. Soc. Dalton Trans.* **1997**, 2887.
[70] Note that the choice of the *x* and *y* axes in Figure 5 is different from that in the orbital correlation diagrams in Reference [11]. Therefore, b_1 and b_2 in their figure mean b_2 and b_1 in our figure.

Received: April 23, 2002 [F4038]

  0947-6539/02/0820-4707 $ 20.00+.50/0